CHAPTER 4

RESULTS AND DISCUSSION (PART I):

Lead Zirconate Titanate (PZT)

In this chapter, the results are presented of the investigation of both powder and ceramic forms of lead zirconate titanate (PZT) which is one of the end components of the PZT-PMN system. Phase formation-structure-processing relationships are brought out and discussed in terms of phase formation, morphology, particle size, densification, crystal structure, microstructural and dielectric properties. Attention is first paid to the ZT precursor, before moving on to the PZT component.

Before embarking on the fabrication of PZT ceramics, it is appropriate here to focus initially on the preparation of PZT powders. A perovskite-like phase of lead zirconate titanate (PZT) powders has been synthesised by employing the intermediate precursor $ZrTiO_4$ (ZT). At the first step, the synthesis of single-phase ZT powder has been performed with formation of $ZrTiO_4$ phase investigated as a function of calcination conditions by DTA, XRD and SEM techniques.

4.1 Zirconium Titanate Powder

4.1.1 Thermal Analysis

A DTA curve obtained for a powder mixed in the stoichiometric proportions of $ZrTiO_4$ is shown in Fig. 4.1. Two exothermic peaks with maxima at 1150 and 1240 ^oC, and two endothermic peaks centered at ca. 1200 and 1270 ^oC were observed in

this profile. It is to be noted that there is no obvious interpretation of the peaks although it is likely to correspond to a phase transition reported by a number of workers.[81-85] These data were used to define the range of temperatures for XRD investigation to between 1100 and 1350 ^{o}C.

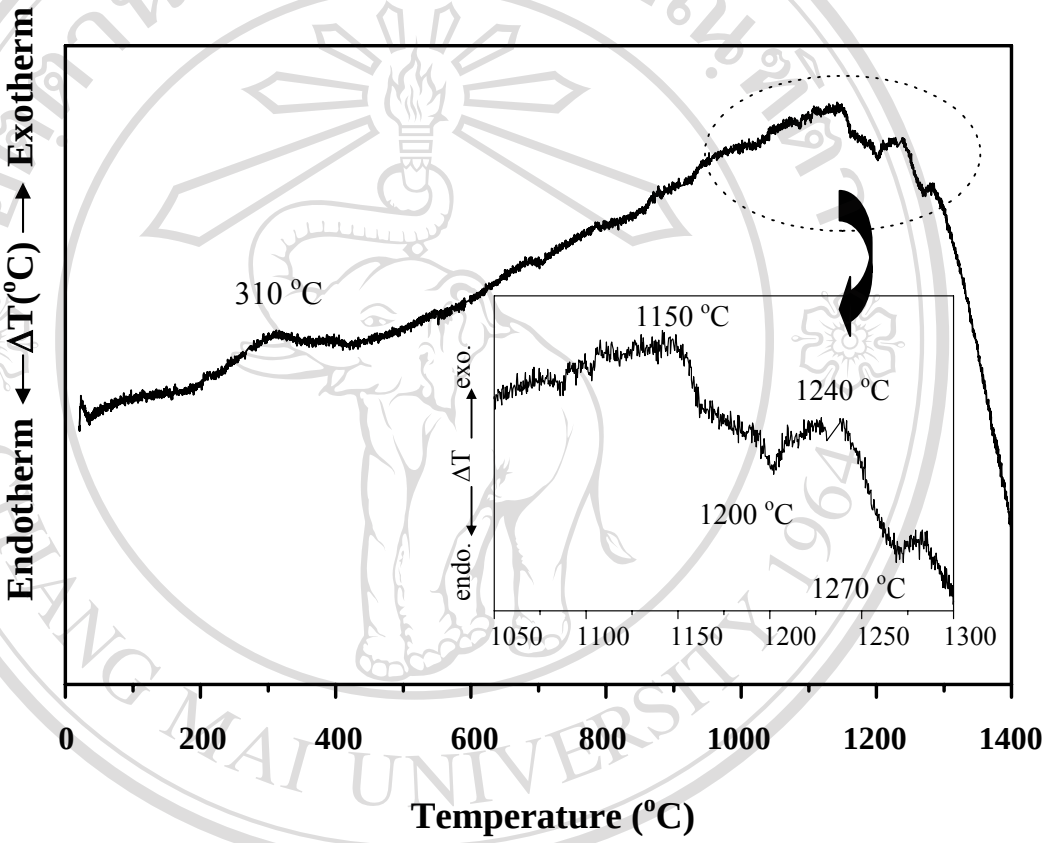

Fig. 4.1 A DTA curve for the mixture of ZrO_2 – TiO_2 powders.

4.1.2 Phase Analysis

All calcined powders, together with that of the starting powder mixtures were examined by XRD in order to investigate the phase development (Figs. 4.2-4.4). In general, the strongest reflections apparent in the majority of the XRD patterns indicate the formation of zirconium titanate phase, $ZrTiO_4$, which can be matched with JCPDS file no. 34-415 (Fig. 4.2). To a first approximation, this major phase has orthorhombic

structure, space group *Pnab* (no. 60), with cell parameters a = 503 pm, b = 549 pm and c = 480 pm.[86] It is also of interest that no evidence has been obtained for the existence of the α-PbO_2-like orthorhombic phase (space group *Pcnb*) reported by Newnham.[87] Depending on the calcination conditions, at least four minor phases were identified, i.e. monoclinic-ZrO_2 (*), tetragonal-ZrO_2 (v), anatase-TiO_2 (o) and rutile-TiO_2 (+), which can be correlated with JCPDS file numbers 37-1484[88], 17-923[89], 21-1272[90] and 21-1276[91], respectively. The precursor ZrO_2 has a baddeleyite-type structure with monoclinic unit cell (a = 531 pm, b = 521 pm, c = 514 pm and β = 99.22°), space group $P2_1/a$ (no.14), whereas tetragonal symmetry (a = 378 pm and c = 951 pm) is associated with anatase-TiO_2 precursor, space group $I4_1/amd$ (no. 141). Both minor phases found in the calcined ZT powders of ZrO_2 and TiO_2 have tetragonal symmetry with unit cell parameters: a = 512 pm and c = 525 pm, space group *P4m2* (no. 115), and a = 378 pm and c = 951 pm, space group $P4_2/mnm$ (no. 136), respectively. It is well established that there are a number of polymorphic forms of ZrO_2 and TiO_2 stable at different temperatures and pressures.

In the present results, monoclinic/tetragonal transformation of ZrO_2 and the anatase/rutile transformation of TiO_2 have been observed. Monoclinic zirconia (*) is detected from the original mixture up to 1200 °C, whereas partial conversion to tetragonal zirconia (v) was observed after heating at 1100 °C, which is associated to the DTA exothermic effect previously observed in Fig. 4.1. It is seen that completed conversion of anatase-TiO_2 (o) precursor to rutile (+) was found after calcination at 1100 °C, in agreement with other work.[92, 93] Neither evidence of $ZrTi_2O_6$ nor indication of the orthorhombic phase of $Zr_5Ti_7O_{24}$ was presented.[94]

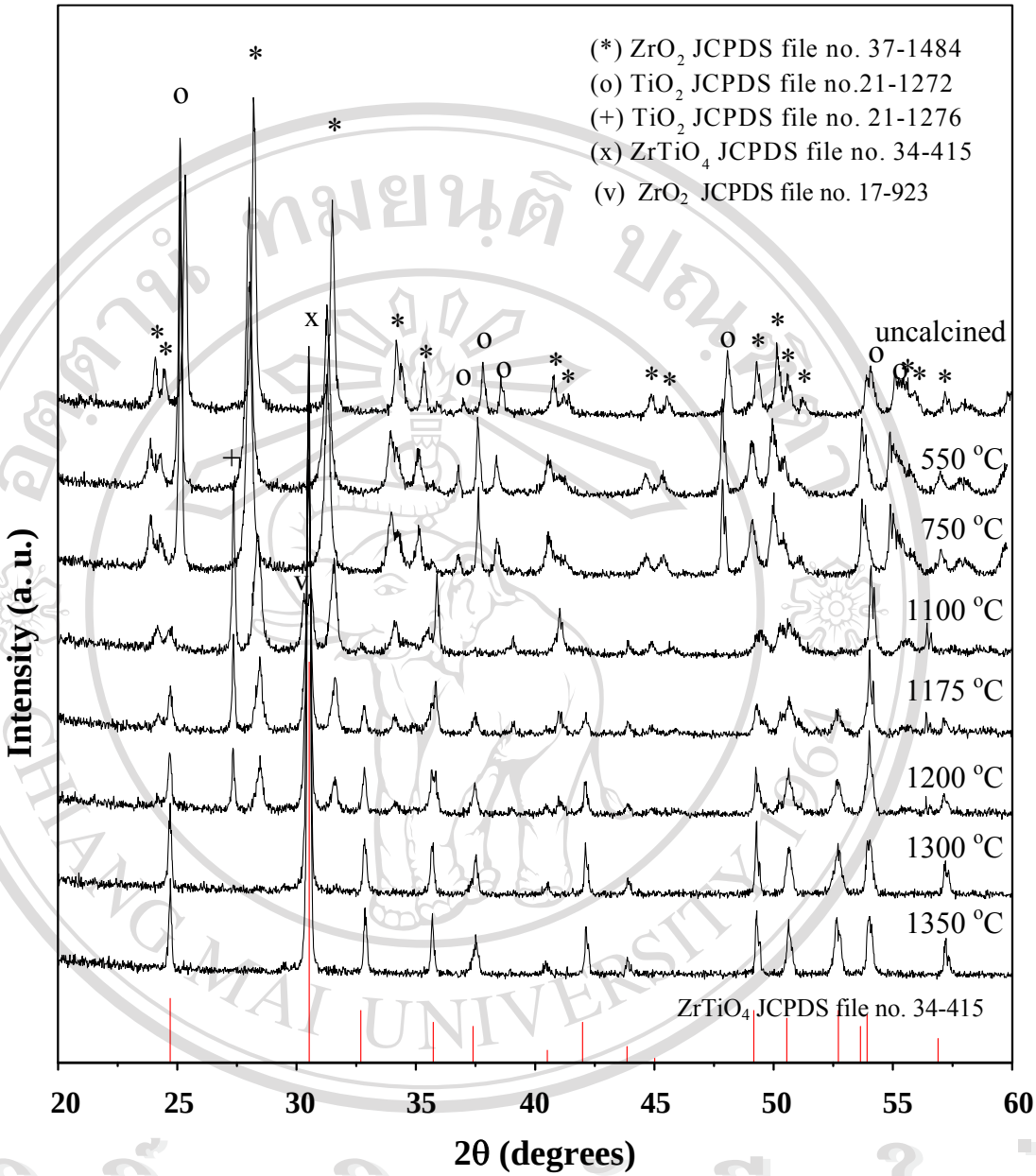

Fig. 4.2 XRD patterns of ZT powder calcined at various temperatures for 4 h with heating/cooling rates of 20 °C/min.

This study shows that minor amounts of the ZrO_2 and TiO_2 phases tend to co-exist along with the zirconium titanate ($ZrTiO_4$) phase, after calcinations in the range 1100-1200 °C. By increasing the calcination temperature, the yield of $ZrTiO_4$

phase increases significantly until 1300 ^{o}C, whereafter higher temperatures do not enhance the yield (Fig. 4.2). Apart from the calcination temperature, the effect of dwell time was also found to be quite significant (Fig. 4.3). It is seen that the single phase of $ZrTiO_4$ (yield of 100% within the limitations of the XRD technique) was found to be possible only in powders, calcined at 1300 ^{o}C with dwell time of 4 h and 6 h.

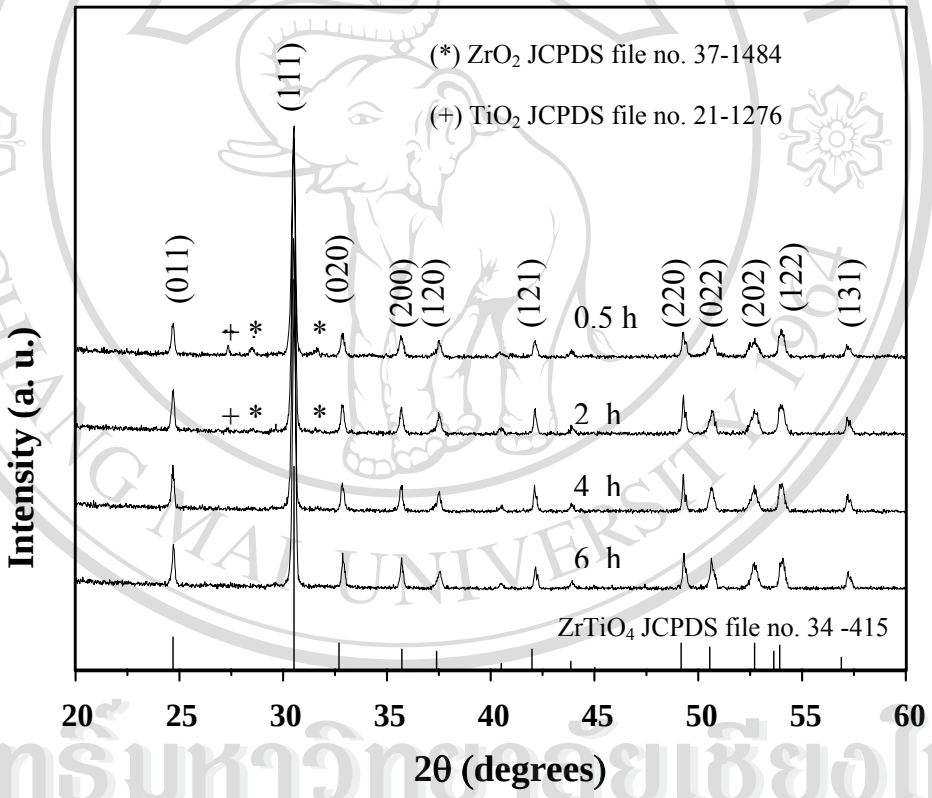

Fig. 4.3 XRD patterns of ZT powder calcined at 1300 ^{o}C with heating/cooling rates of 20 ^{o}C/min for various dwell times.

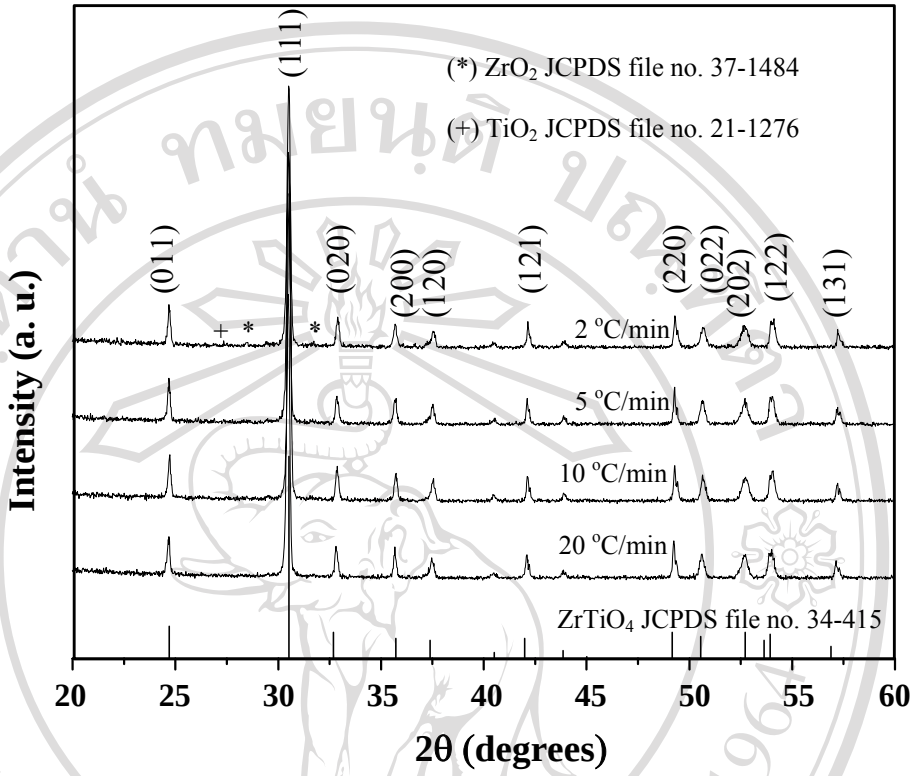

Fig. 4.4 XRD patterns of ZT powder calcined at 1300 °C for 4 h with various heating/cooling rates.

In the present study, an attempt was also made to calcine ZT powders under various heating/cooling rates (Fig. 4.4). In this connection, it is shown that the yield of $ZrTiO_4$ phase did not vary significantly with different heating/cooling rates ranging from 5 to 20 °C/min. It is to be noted that doublets observed in the XRD pattern for $ZrTiO_4$ at $2\theta = 48^o$, 50^o, 52^o, 54^o and 57^o (heating/cooling rates of 2 °C/min) could be attribute to the formation of minor phase $Zr_5Ti_7O_{24}$. This phase also has the α-PbO_2 type structure and a well-define superstructure with a tripled *a*-axis.[95] It is well established that zirconium titanate-based sample exhibiting difference degrees of

ordering may be generated by employing high temperature treatment and different heating/cooling rates.[95]

Based on the DTA and XRD data, it may be concluded that, over a wide range of calcination conditions, single phase $ZrTiO_4$ cannot be straightforwardly formed via a solid state mixed oxide synthetic route. Between 1100 and 1150 ^oC, TiO_2 anatase is transformed into the rutile phase. After 1200 ^oC, ZrO_2 totally disappeared yet, up to 1240 ^oC, TiO_2 is remaining. A large temperature decrease observed at temperature greater than 1275 ^oC may be attributed to the crystallization of $ZrTiO_4$. The experimental work carried out here suggests that the optimal calcination conditions for single phase $ZrTiO_4$ is 1300 ^oC for 4 h with heating/cooling rates as fast as 20 ^oC/min.

4.1.3 Morphological Analysis

The morphological evolution during calcination was investigated by SEM. Micrographs of ZT powders calcined at various temperatures from 1100 to 1300 ^oC for 4 h are shown in Fig. 4.5. In general, the particles are agglomerated and basically irregular in shape, with a substantial variation in particle size, particularly in samples calcined at high temperatures. The range of particle diameter was found to be about 0.2-1.0, 0.2-1.5, 0.3-2.0 and 0.5-3.0 μm for the samples calcined at 1100, 1175, 1200 and 1300 ^oC for 4 h, respectively. The results indicate that averaged particle size and degree of agglomeration tend to increase with calcination temperature. Moreover, the grain shape exhibits greater sphericity at higher temperatures.

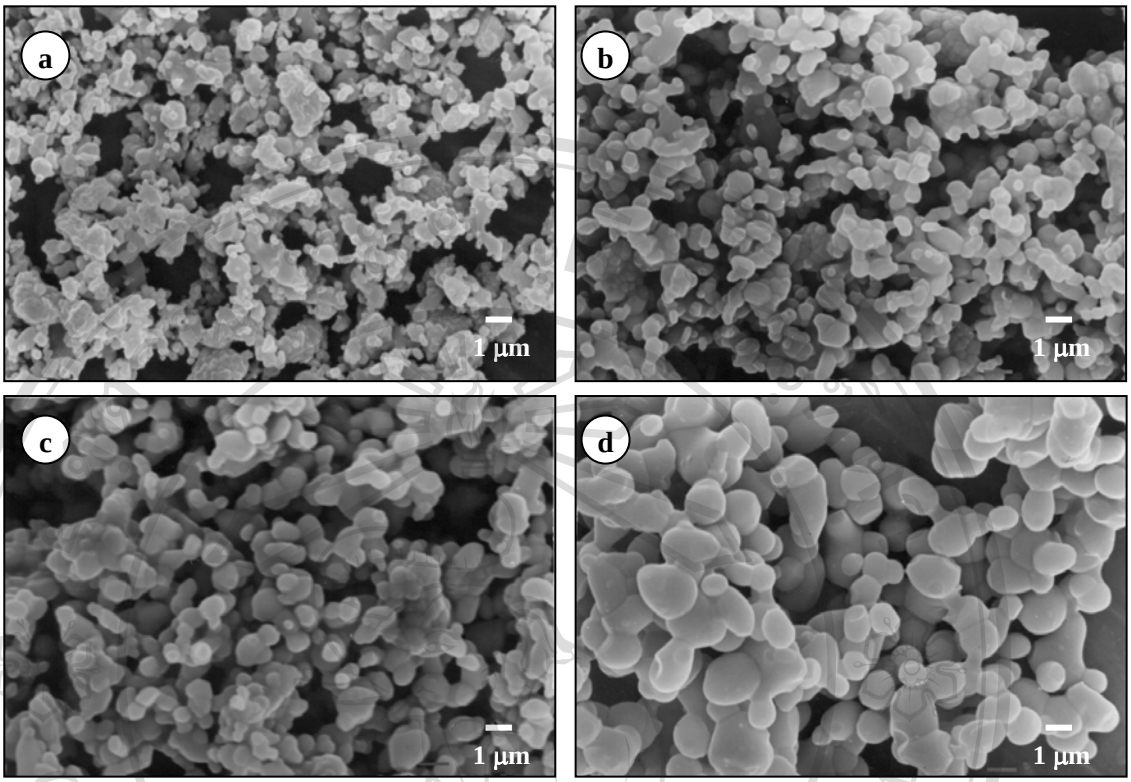

Fig. 4.5 SEM micrographs of the calcined ZT powders at (a) 1100 ^{o}C, (b) 1175 ^{o}C, (c) 1200 ^{o}C and (d) 1300 ^{o}C for 4 h with heating/cooling rates of 20 ^{o}C/min.

Single-phase of ZT powders can be produced by employing a solid state reaction process using oxides as starting materials. Evidence has been obtained for a 100% yield of an orthorhombic $ZrTiO_4$ at a calcination temperature of 1300 ^{o}C for 4 h with heating/cooling rates of 20 ^{o}C/min. The resulting ZT powders consist of agglomerated particles of 0.5 to 3.0 μm in size.

4.2 Lead Zirconate Titanate Powder

In this work, a modified, two-stage mixed oxide synthetic route for preparing high purity PZT powders has been developed. To ensure a single-phase perovskite formation, an intermediate phase of zirconium titanate ($ZrTiO_4$) derived from section 4.1 was employed as starting precursors. The formation of perovskite phase in the calcined PZT powder has been investigated as a function of calcination temperature, soaking time and heating/cooling rates by DTA and XRD techniques as described here.

4.2.1 Thermal Analysis

A DTA curve obtained for a powder mixed in the stoichiometric proportions of PbO and $ZrTiO_4$ is shown in Fig. 4.6. In the temperature range 200-400 ^oC, the sample shows several large exothemic peaks in the DTA curve. These DTA peaks can be attributed to the decomposition of the organic species from the milling process. The different temperature, intensities, and shapes of the thermal peaks probably are related to the different natures of the organic species and consequently, caused by the removal of species differently bounded in the network.

In the temperature range 700-1000 ^oC, both exothermic and endothermic peaks are observed in the DTA curve. The enlarge zone of this DTA curve shown that the exothermic peak centered at ~ 780 ^oC may result from perovskite phase crystallization and that is also in accordance to literature data.[28, 32, 40, 96] The last endothermic peak centered at ~ 840 ^oC may be caused by the decomposition of lead oxide. These temperatures have been obtained from the calibration of the sample thermocouple and were used to define the range of temperatures (700-950 ^oC),

soaking time (0.5 to 2 h) and heating/cooling rates (5 to 20 ^{o}C/min) for the XRD investigation.

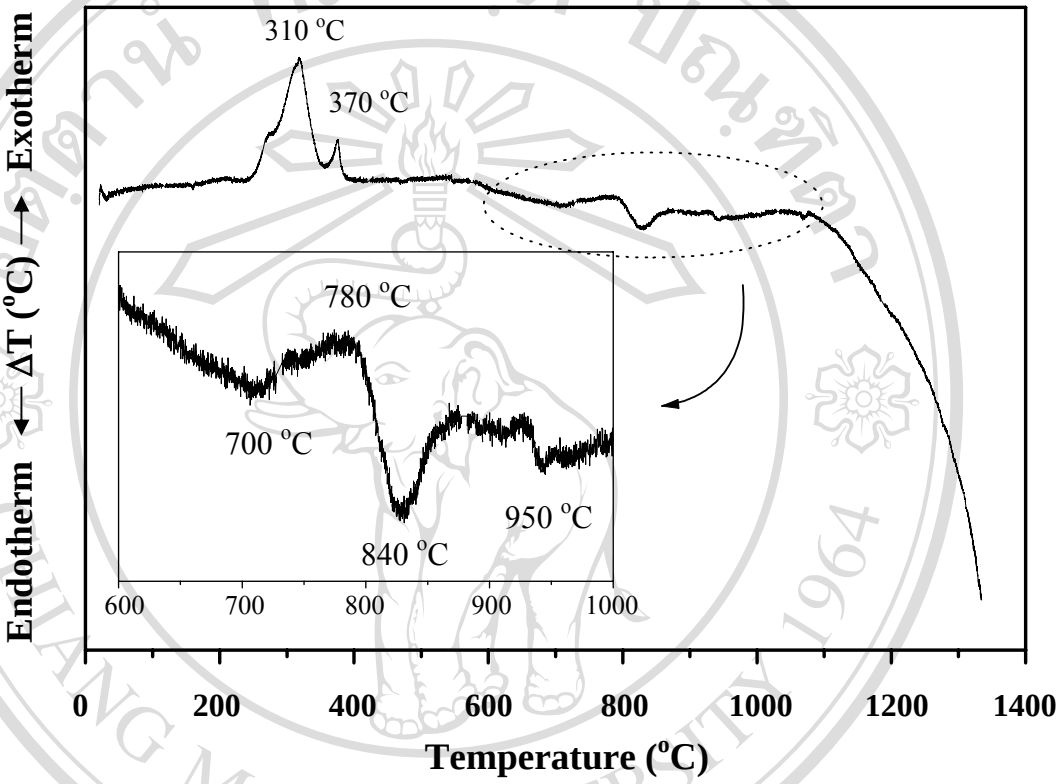

Fig. 4.6 A DTA curve for the mixture of PbO-$ZrTiO_4$ powders.

4.2.2 Phase Analysis

Powder XRD patterns of the calcined powders are given in Figs. 4.7-4.12, with the corresponding JCPDS patterns also shown. The optimum calcination temperature for the formation of a high purity PZT phase was found to be about 760 ^{o}C, i.e. slightly lower than the exothermic temperature in Fig. 4.6. In general, the strongest reflections apparent in the majority of the XRD patterns indicate the formation of two lead zirconate titanate phases. These can be matched with JCPDS

file numbers 50-346[97] and 73-2022[98] for the tetragonal $Pb(Zr_{0.44}Ti_{0.56})O_3$ and rhombohedral $Pb(Zr_{0.52}Ti_{0.48})O_3$ (Fig. 4.8), respectively. As is well known, the variations in composition may lead to a diffuse MPB between the tetragonal and rhombohedral PZT phase.[99] The most obvious different between the patterns for tetragonal and rhombohedral PZT phases concerns the presence of a splitting of (002)/(200) peak at two-theta about 43^o-45^o for the former phase (Fig. 4.9).

It is seen that, with the exception of powder calcined at 950 ^oC, the rhombohedral PZT phase is always present in the product. Moreover, some additional weak reflections are found in the XRD patterns (marked by + and x), which correlate with the precursors PbO and $ZrTiO_4$, respectively (Figs. 4.7, 4.11 and 4.12). For the purpose of estimating the concentrations of the phases present, Eq. 3.5 (*see Chapter 3*) has been applied to the powder XRD patterns obtained as given in Table. 4.1. This study shows that minor amount of the unreacted PbO and $ZrTiO_4$ phases tends to co-exist along with the PZT phase, after scanning calcination in the temperature range 700-740 ^oC. Upon calcination at 760 ^oC, the phases of PbO and $ZrTiO_4$ have been found completely disappear, and crystalline PZT of both tetragonal and rhombohedral is the only detectable phases in the powder.

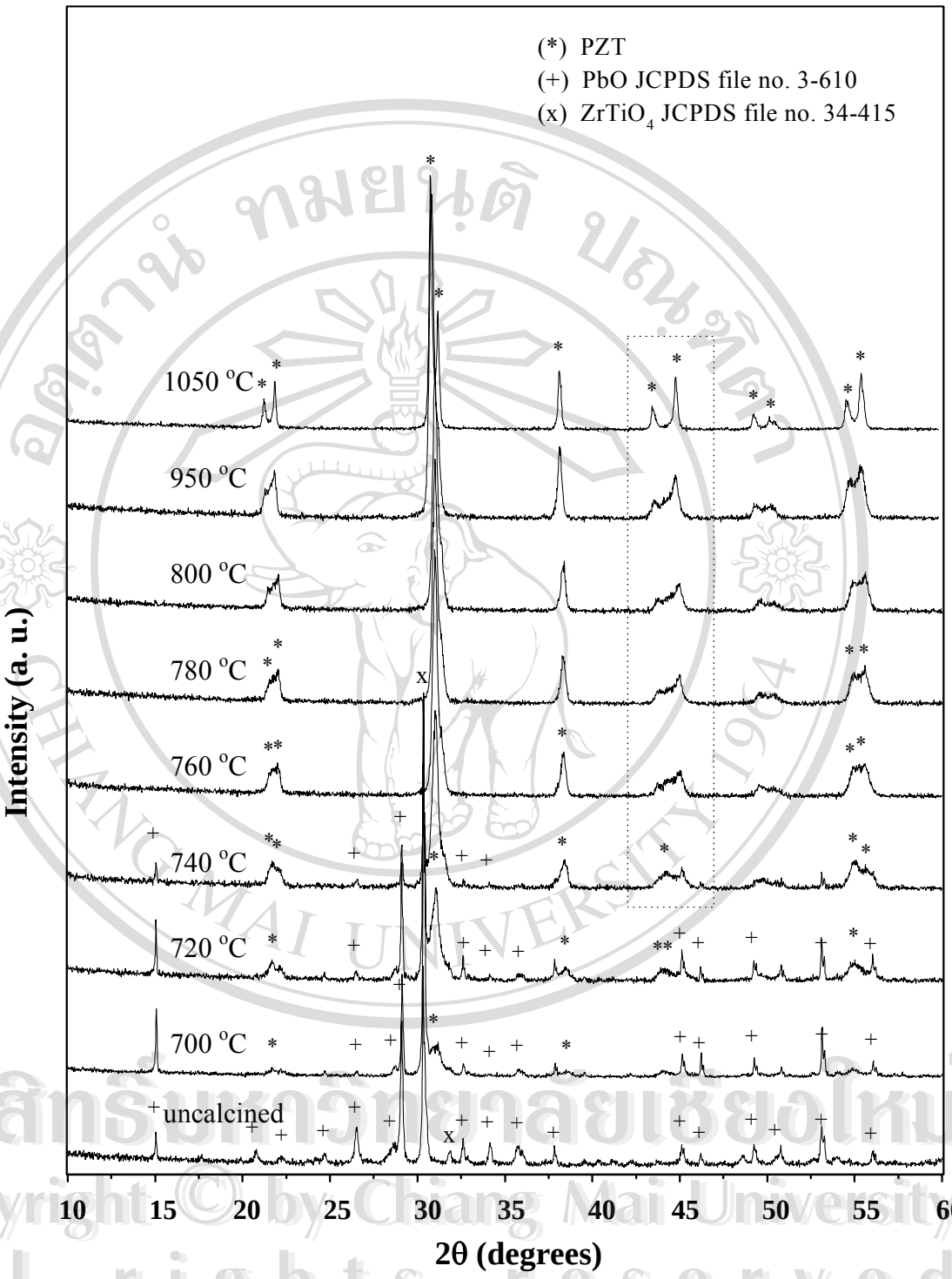

Fig. 4.7 Powder XRD patterns of the calcined PZT powders at various calcination temperatures for 2 h with heating/cooling rates of 20 °C/min.

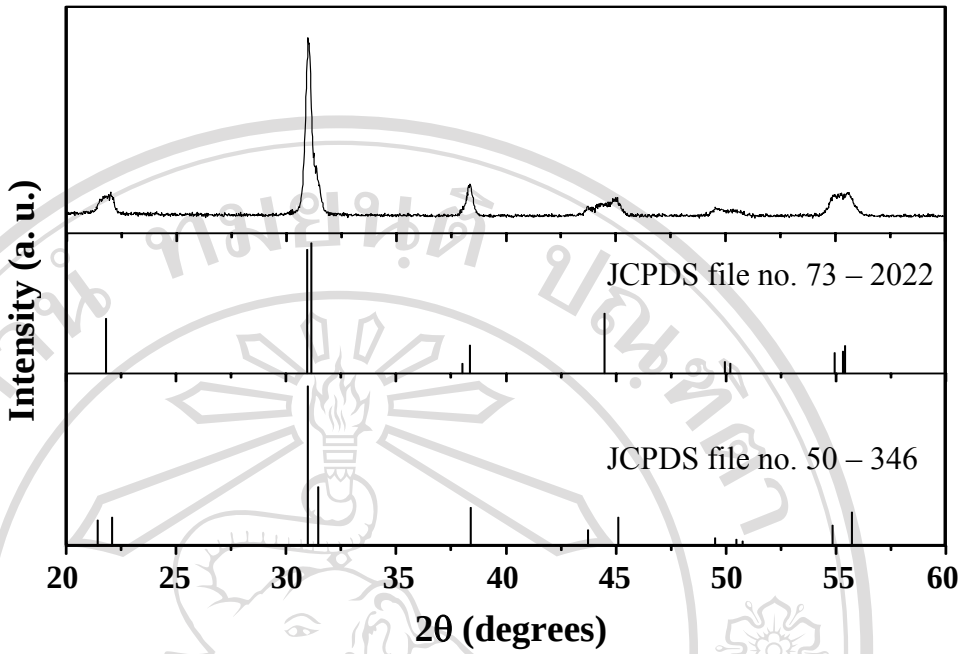

Fig. 4.8 Computerised JCPDS data-matching confirms that formation of both tetragonal and rhombohedral PZT phases in the calcined powder.

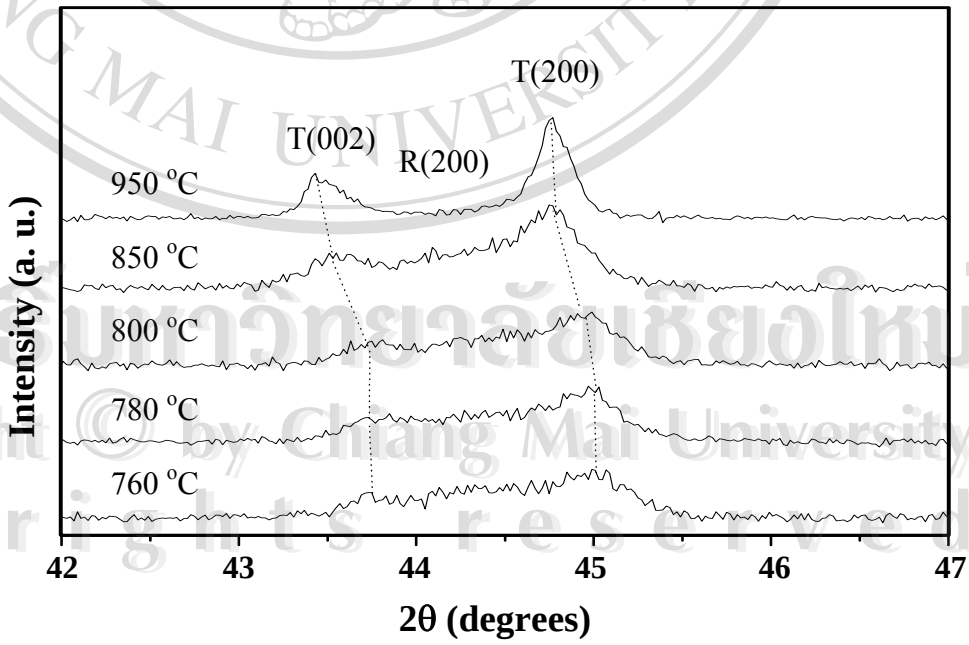

Fig. 4.9 Enlarged XRD peaks for the tetragonal (T) and rhombohedral (R) phases as a function of calcination temperatures (dotted line in Fig. 4.7).

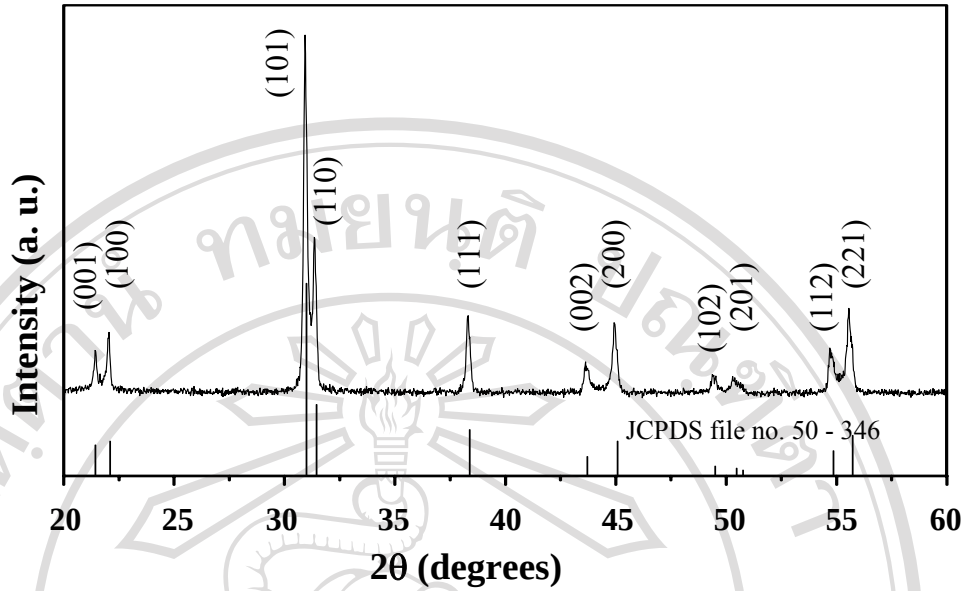

Fig. 4.10 Computerised JCPDS data-matching confirms that formation of the single-phase tetragonal PZT.

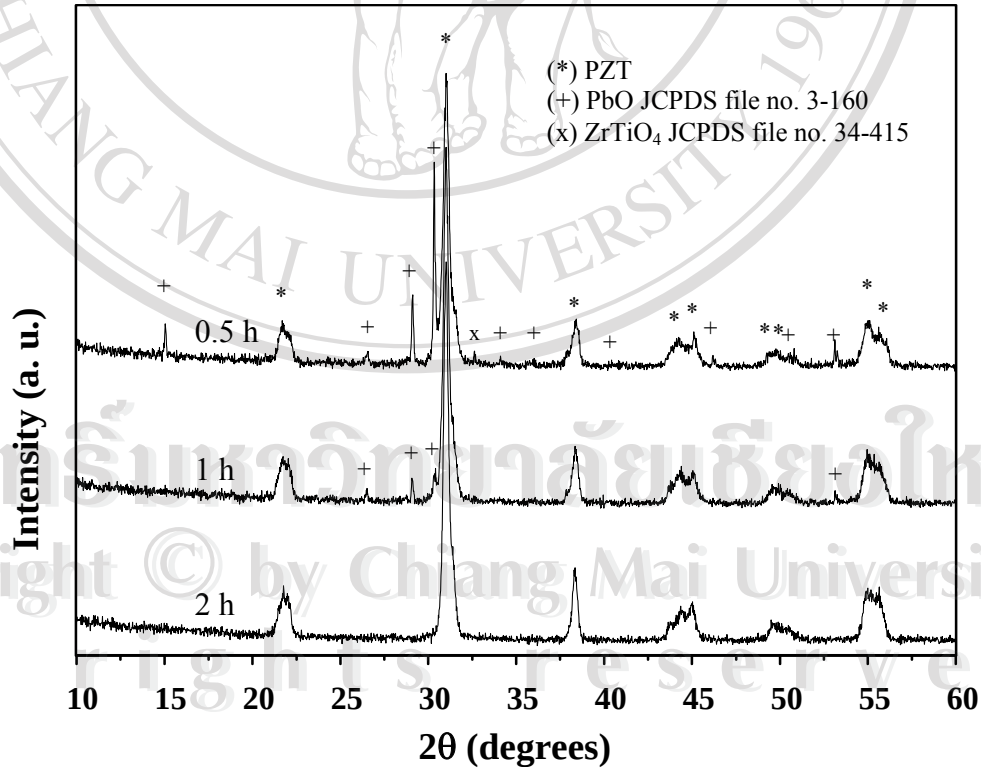

Fig. 4.11 Powder XRD patterns of the PZT powders calcined at 760 ^{o}C with heating/cooling rates of 20 ^{o}C/min for various dwell times.

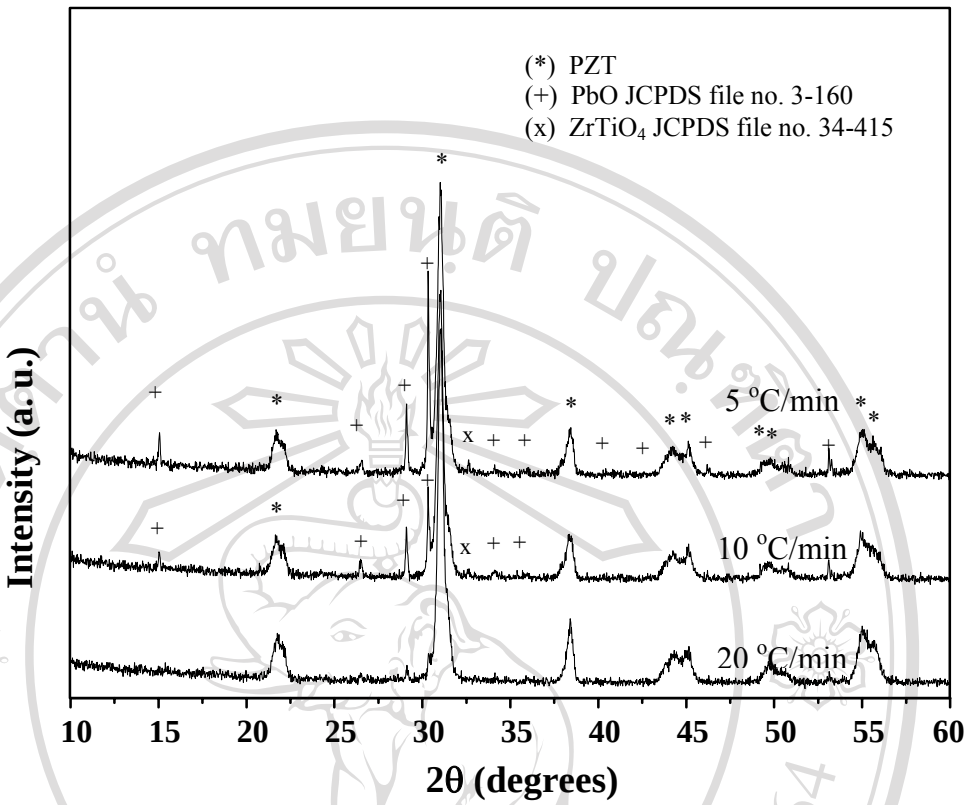

Fig. 4.12 Powder XRD patterns of the PZT powders calcined at 760 °C for 2 h with various heating/cooling rates.

By increasing the calcination temperature from 760 to 950 °C, the yield of the tetragonal PZT phase increases significantly until at 950 °C, a single phase of tetragonal PZT is formed (Fig. 4.10) Neither lead titanate ($PbTiO_3$) or lead zirconate ($PbZrO_3$) earlier reported by Chakrabarti and Maiti [100] has been found in this study. It is also of interest to point out that no evidence has been obtained for the existence of pyrochlore phase $Pb_2Ti_2O_7$ and unreacted ZrO_2 reported by Branković et al.[33] The effects of soaking time and heating/cooling rates on phase formation were found to be quite significant (Figs. 4.11 and 4.12). In this work, it is seen that the optimum soaking time and heating/cooling rates for the formation of a high purity PZT phase were found to be at 2 h and 20 °C/min, respectively. Therefore, XRD results clearly

show that, in general, the methodology presented in this work provides a simple method for preparing perovskite PZT powders via a modified solid-state mixed oxide synthetic route without the addition of PbO in excess.[51, 101] It is interesting to note that the use of zirconium titanate precursor together with the milling technique can effectively enhance the yield of the PZT phase.

Table 4.1 Calculated PZT phases as a function of calcination conditions.

Calcination conditions			Qualitative concentrations of PZT phase	
Temperature (^{o}C)	Time (h)	Rates (^{o}C/min)	Tetragonal (wt.%)	Rhombohedral (wt.%)
700	2.0	20	*	*
720	2.0	20	*	*
740	2.0	20	*	*
760	0.5	20	*	*
760	1.0	20	*	*
760	2.0	5	*	*
760	2.0	10	*	*
760	2.0	20	60	40
780	2.0	20	64	36
800	2.0	20	72	28
850	2.0	20	79	21
900	2.0	20	87	13
950	2.0	20	100	0

The estimated precision of the concentration values for the two phases is ± 0.1 %.

* PZT, PbO and $ZrTiO_4$ phases were found and Eq. (3.5) is not valid.

4.2.3 Morphological Analysis

The morphological changes in the PZT powders formed by a modified two-stage mixed oxide are illustrated in Fig. 4.13 as a function of formation temperature. After calcinations at 700 to 950 ^{o}C, the powders have similar morphology. They had spherical secondary particles composed of submicrometer-sized primary particulates. This structure is similar to that of $BaTiO_3$ powders synthesised by previous researchers.[102]

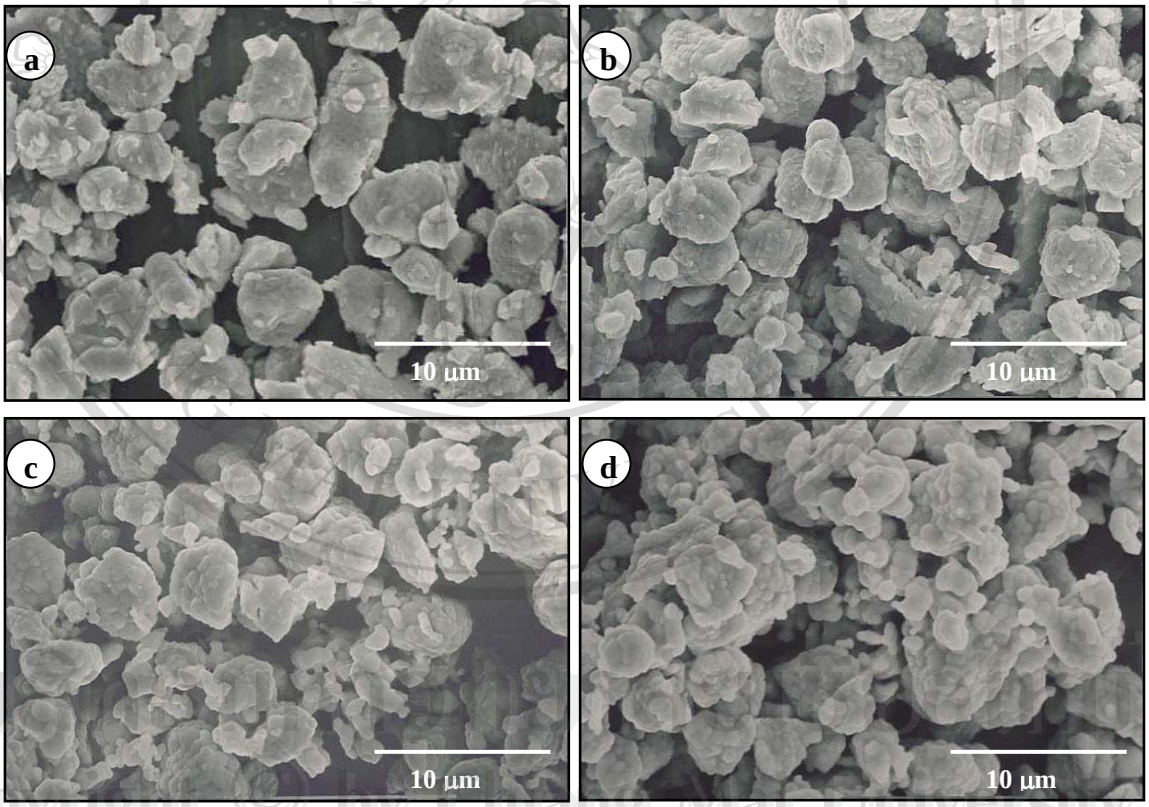

Fig. 4.13 SEM micrographs of the PZT powders calcined at (a) 700 ^{o}C, (b) 740 ^{o}C, (c) 760 ^{o}C and (d) 950 ^{o}C.

The primary particles have sized of about 0.05-0.20 μm, and the agglomerates particles about 1.0-8.0 μm. At 700 ^{o}C, three phases (PbO, $ZrTiO_4$ and PZT) were observed in X-ray diffraction analysis (Fig. 4.7), but from the SEM micrograph (Fig. 4.13), it was difficult to distinguish these three phases because of the lumpy particle morphology, indicating significant growth interaction in the multiphase composition. By increasing the calcination temperature from 700 to 850 ^{o}C, the mixture of both tetragonal and rhombohedral PZT phases with various sizes of irregular shaped particles (clusters) was observed (Fig. 4.13). Upon futher increases of temperature up to 950 ^{o}C, the tetragonal PZT phase with similar cluster was found. In general, this granule characteristic will offer an apparent advantage towards achieving a high sintered density and homogeneous microstructure of PZT ceramic at a reduced sintering temperature.

4.3 Lead Zirconate Titanate Ceramic

The purpose of this section was to study the phase formation, densification, microstructure and dielectric properties of PZT ceramics fabricated using the pressureless sintering method. Processing variables included deviation from the PZT stoichiometry, sintering temperature, dwell time and heating/cooling rates. Finally, the influence of sintering conditions upon microstructures and dielectric characteristics are emphasized.

4.3.1 Phase Analysis

XRD patterns of PZT ceramics sintered at various temperatures are given in Fig. 4.14. The strongest reflections in the majority of the XRD patterns indicate

formation of the perovskite phase of the composition $Pb(Zr_{0.44}Ti_{0.56})O_3$, which could be match with JCPDS file no. 50-346.[97] To a first approximation, this phase has a tetragonal perovskite-type structure in space group *P4mm* (no. 99), with cell parameters a = 401 pm and c = 414 pm, respectively. It can be seen that as the sintering temperature increases, the peak intensities have been developed. However, for the sample sintered at 1320 °C, some additional reflections (marked by *) are observed, and these can be identified as presence of ZrO_2 (JCPDS file no. 37-1484).[88] This phase has a monoclinic structure with cell parameters a = 531.2 pm, b = 521.2 pm, c = 514.7 pm and β = 99.218º in space group $P2_1/a$ (no. 14). Compositional fluctuations due to the evaporation of lead oxide within surface regions are believed to be responsible for the occurrence of free ZrO_2 phase in sample sintered at 1320 °C. Another possibility was explained by Fushimi and Ikeda (Fig. 2.3),[103] who suggested that melting of PT-PZ solid solution can change from congruent to incongruent and induce ZrO_2 to form at ~ 1340 ^oC. On the other hand, Branković et al.[33] suggested that incomplete reaction of the starting precursors can also result in the persistance of free ZrO_2 or PbO phases. Due to no trace of ZrO_2 has been observed for the samples sintered at the temperatures below 1320 ^oC. For the present result, it is believed that the consequence of PbO evaporation is an apparently favorable factor in facilitating the occurrence of ZrO_2 at a higher sintering temperature.

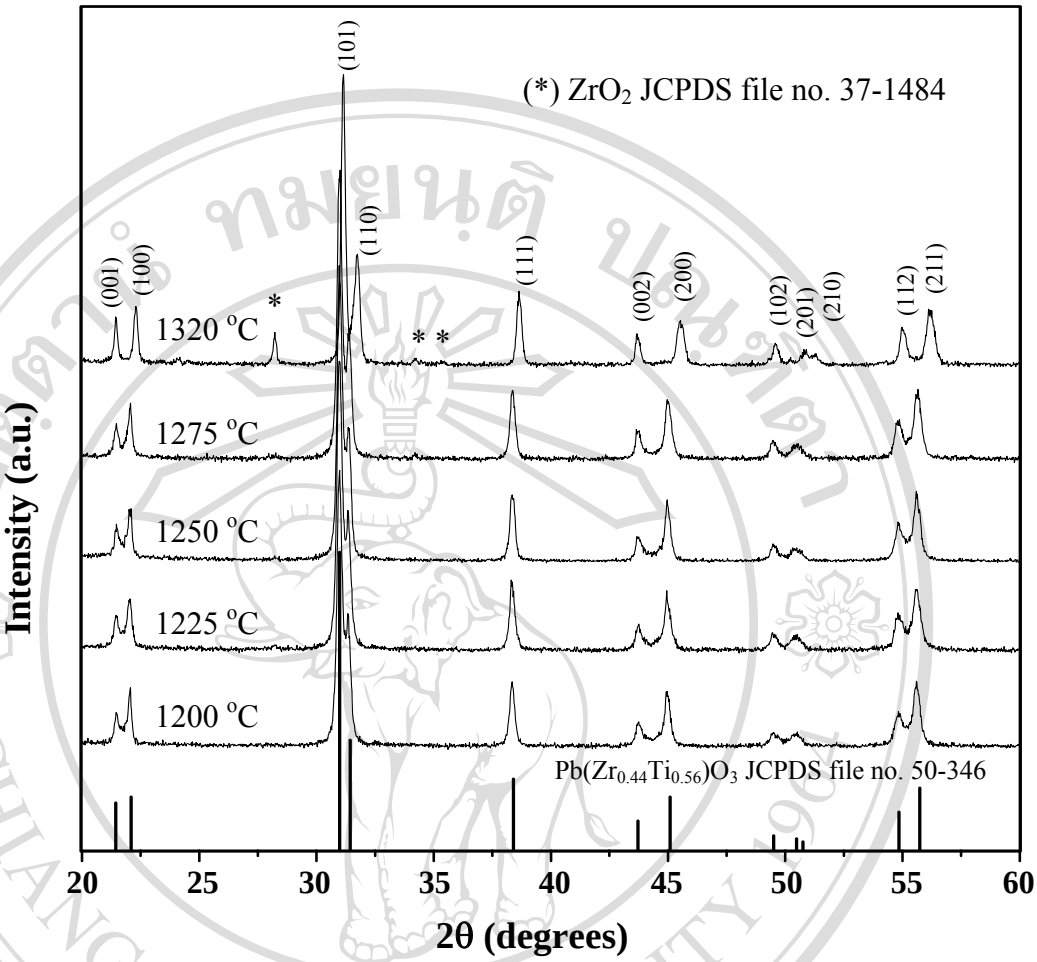

Fig. 4.14 XRD patterns of PZT ceramics sintered at various temperatures for 4 h with heating/cooling rates of 10 °C/min.

To identified the chemical composition of each phase, a combination of back scattering electron imaging (BEI) and energy dispersive spectroscopy (EDS) was conducted on the samples sintered at 1275 °C. As shown in Fig. 4.15, the presence of inhomogeneous chemical composition in the sintered samples is indicated by a relatively dark and gray color-grains. These grains should have a different chemical composition as seen in the result of the EDS analysis, which is suggest that the darker grains are due to presence of ZrO_2. Thus, segregation of ZrO_2 observed in this

particular sample may be associated with loss of Pb content. However, there is no presence of ZrO_2 in other samples that sintered at lower temperature, i.e 1200 ^oC and 1250 ^oC for 4 h with heating/cooling rates of 10 ^oC/min.

Table 4.2 is the summary of EDS analysis taken from the PZT sample sintered at 1275 °C. There are three possible compositions, ZrO_2, $Pb(Zr_{0.45}Ti_{0.53})O_3$ and $Pb(Zr_{0.47}Ti_{0.55})O_3$ that may present in this sample. The observed major phases of the ceramic are $Pb(Zr_{0.45}Ti_{0.53})O_3$ and $Pb(Zr_{0.47}Ti_{0.55})O_3$, respectively. It can be seen that the observed composition is deviated from proposed composition of $Pb(Zr_{0.50}Ti_{0.50})O_3$. For the PZT samples sintered at 1225 and 1250 ^oC for 4 h with heating/cooling rates of 10 ^oC/min, the major phase is the same as identified in the previous two samples. Thus, proposed composition should also be $Pb(Zr_{0.5}Ti_{0.5})O_3$. The results of SEM micrographs also suggest a single phase present in both samples. Since, there is no compositional contrast seen in the SEM micrograph taken with backscattered emission mode. These were confirmed by the EDS analysis. Noticeably, there is no ZrO_2 impurity contained in the latter two samples that sintered at lower temperatures. Thus, segregation of ZrO_2 may be induced by loss of PbO at higher sintering temperature.

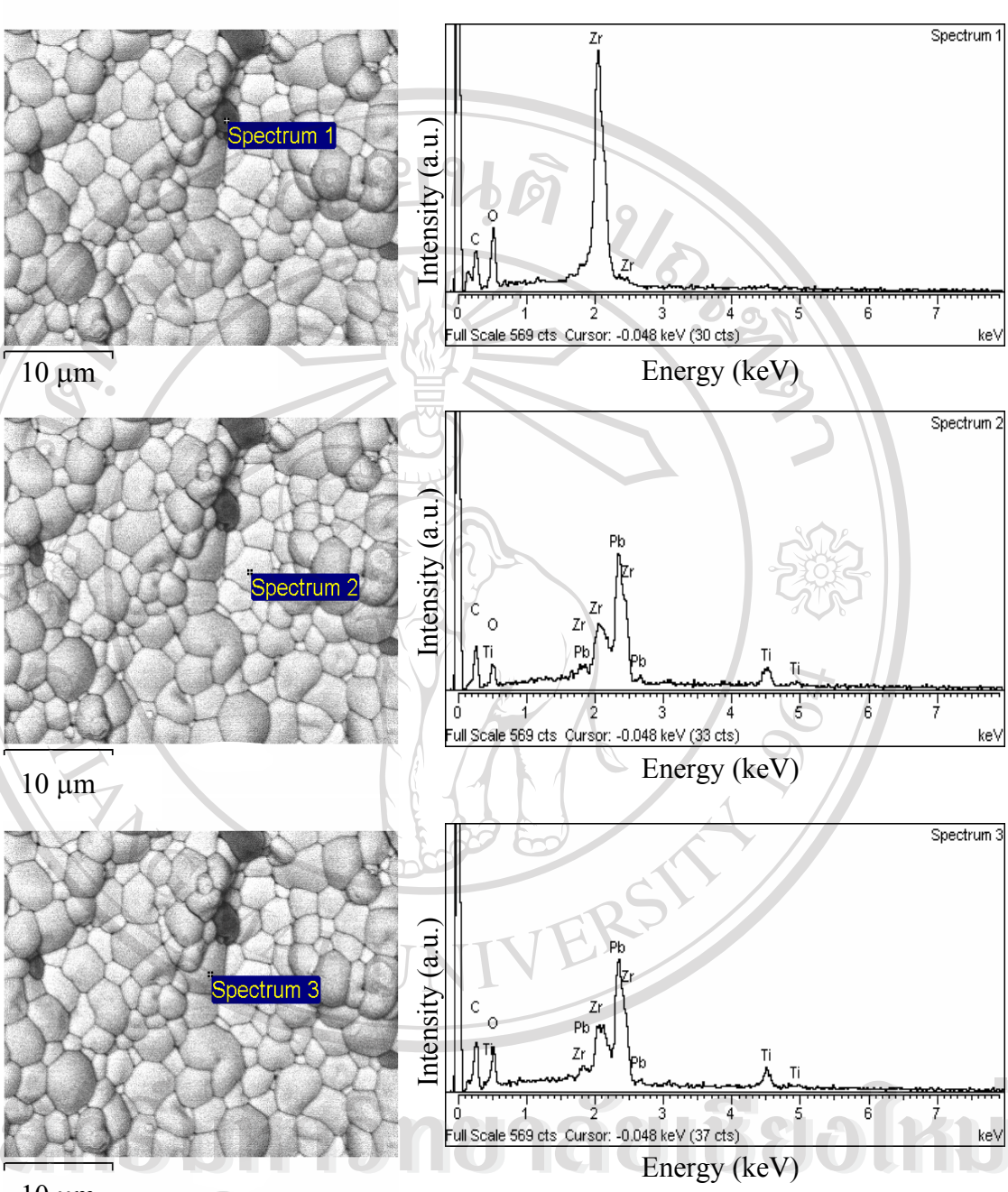

Fig. 4.15 EDS analysis results in three different grains of PZT ceramic sintered at 1275 ^{o}C for 4 h with heating/cooling rates of 10 ^{o}C/min.

Table 4.2 Chemical compositions of the PZT ceramic (sintered at 1275 ^{o}C for 4 h with heating/cooling rates of 10 ^{o}C/min) from EDS analysis.

Spectrum no.	Compositions (at %)			Possible phases
	Ti (K)	Zr (K)	Pb (M)	
1	-	100	-	ZrO_2
2	26.8	22.8	50.4	$Pb(Zr_{0.45}Ti_{0.53})O_3$
3	27.0	23.0	49.0	$Pb(Zr_{0.47}Ti_{0.55})O_3$

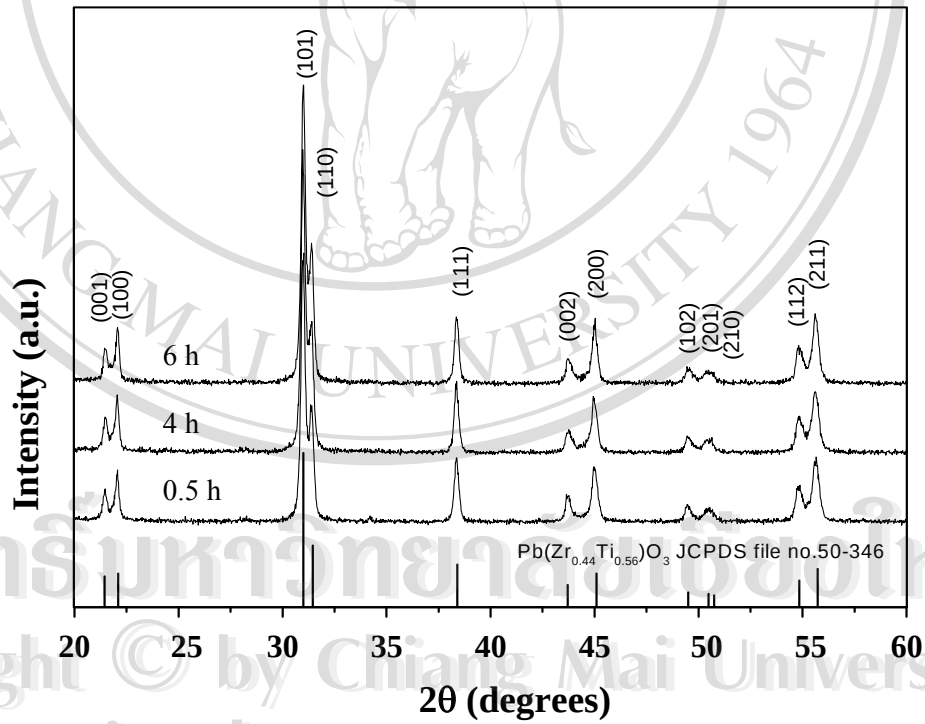

Fig. 4.16 XRD patterns of PZT ceramics sintered at 1250 ^{o}C with heating/cooling rates of 10 ^{o}C/min for various dwell times.

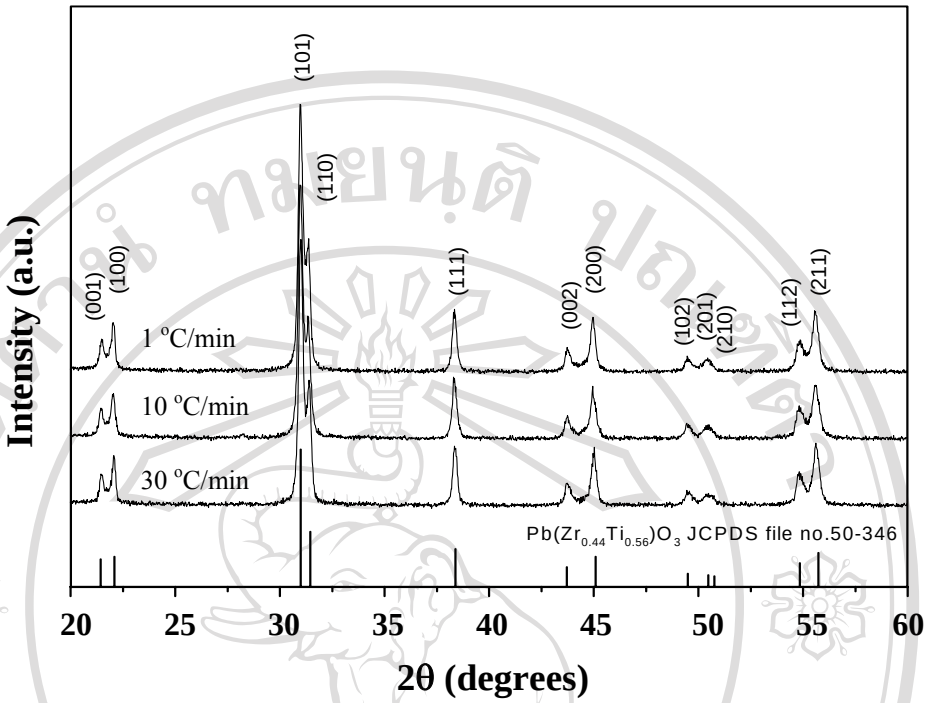

Fig. 4.17 XRD patterns of PZT ceramics sintered at 1250 °C for 4 h with various heating/cooling rates.

The effect of sintering temperature (in the range from 1225 to 1320 °C) on phase formation was found to be insignificant. Only small amounts of ZrO_2 were detected in samples sintered at 1320 °C. A single phase of perovskite PZT (yield of 100% within the limitations of the XRD technique) was obtained in samples sintered at 1100 to 1250 °C. This is probably due to a carefully optimised reaction to form single-phase precursor powders (see section 4.1). Moreover, the degree of lead loss during this selected sintering scheme is probably below the certain level which normally leads to pyrochlore formation as suggested by other workers.[104, 105]

Apart from the sintering temperature, the effects of dwell times (0.5-6 h) and heating/cooling rates (1-30 °C/min) were also found to be insignificant (Figs. 4.16 and

4.17). In this work, it is seen that the optimum dwell time and heating/cooling rates for the formation of a high purity PZT ceramics were found to be at 0.5 h and 30 ^{o}C/min, respectively. Therefore, XRD results inconnection with EDS analysis clearly show that, in general, the methodology presented in this work provides a simple method without the addition of PbO in excess.[37, 106, 107] The effect of sintering temperature on the phase formation was pronounced especially at higher temperature. It was demonstrated that ceramics sintered at 1320 ^{o}C exhibited a coexistence of ZrO_2 and PZT phase as a result of chemical heterogeneity. However, the only information from phase identification is not sufficiently to make an intensive summary of the optimised firing conditions for the fabrication of PZT ceramics, further information obtained from other studies is required as described in the following section.

4.3.2 Densification and Microstructural Analysis

In this section, densification of the PZT for various sintering conditions is investigated. Density, shrinkage and average grain size data of all PZT ceramics sintered at various conditions are given in Tables 4.3 and 4.4. It is observed that a density of about 78-97% of the maximum value of PZT* can be achieved in this study. The change in density versus the sintering temperature (1100-1320 ^{o}C) is given in Fig. 4.18.

* The theoretical density of tetragonal phase of PZT ceramics was estimated from the lattice parameter data to be ~ 8.006 g/cm^3 (JCPDS file no 33-784).[118]

The sintered density increases with rising temperature over the range from 1100 to 1250 ^{o}C, where it maximizes. The sintering temperature (1250 ^{o}C) at which a maximum sintered density of ~ 97% theoretical density is obtained compares favorably to those of Wang et al.'s work [101] where sintering aids of Li_2CO_3, Bi_2O_3 and CuO have been used. The increasing sintered density with rising temperature at < 1250 ^{o}C may be explained by the enhanced densification as the sintering temperature for PZT is normally around 1200 ^{o}C.[106] Further increase in the sintering temperature causes a decrease in density values. This may be attribute to the loss of lead oxide at high sintering temperatures, which is similar to the results of other Pb-based perovskite systems.[107, 108]

Table 4.3 Effect of sintering temperatures on phase formation and densification in sintered PZT ceramics.

Sintering temperature (^oC)	Dwell time (h)	Heating/cooling rates (^oC/min)	Perovskite (wt%)	Relative* Density (%)	Shrinkage** (%)	Average*** Grain size (μm)
1100	4	10	100	78.3	5.9	1.20
1150	4	10	100	89.1	10.6	1.53
1200	4	10	100	95.9	12.9	1.84
1225	4	10	100	96.7	13.8	2.26
1250	4	10	100	97.3	13.1	2.76
1275	4	10	98.33	96.4	12.8	3.16
1290	4	10	79.45	96.2	12.2	/

* The estimated precision of the relative density is ± 0.2 % ** The estimated precision of the linear shrinkage is ± 0.2 %

*** The estimated precision of an average grain size is ± 0.1 μm

/ The average grain size can not be estimated due to the coexistence of ZrO_2 phase.

Table 4.4 Effect of dwell time and heating/cooling rates on phase formation and densification in PZT ceramics sintered at 1250 ^{o}C.

Sintering temperature (^{o}C)	Dwell time (h)	Heating/cooling rates (^{o}C/min)	Perovskite (wt%)	Relative* Density (%)	Shrinkage** (%)	Average*** Grain size (μm)
1250	2	10	100	96.0	12.3	2.98
1250	6	10	98.98	92.2	12.8	/
1250	8	10	97.82	86.9	12.9	/
1250	4	1	98.53	96.1	12.4	/
1250	4	5	99.06	96.2	12.6	/
1250	4	20	100	96.9	12.5	4.27
1250	4	30	100	96.9	12.5	4.44

* The estimated precision of the relative density is ± 0.2 %

** The estimated precision of the shrinkage is ± 0.2 %

*** The estimated precision of an average grain size is ± 0.05 μm

/ The average grain size can not be estimated due to the coexistence of ZrO_2 phase.

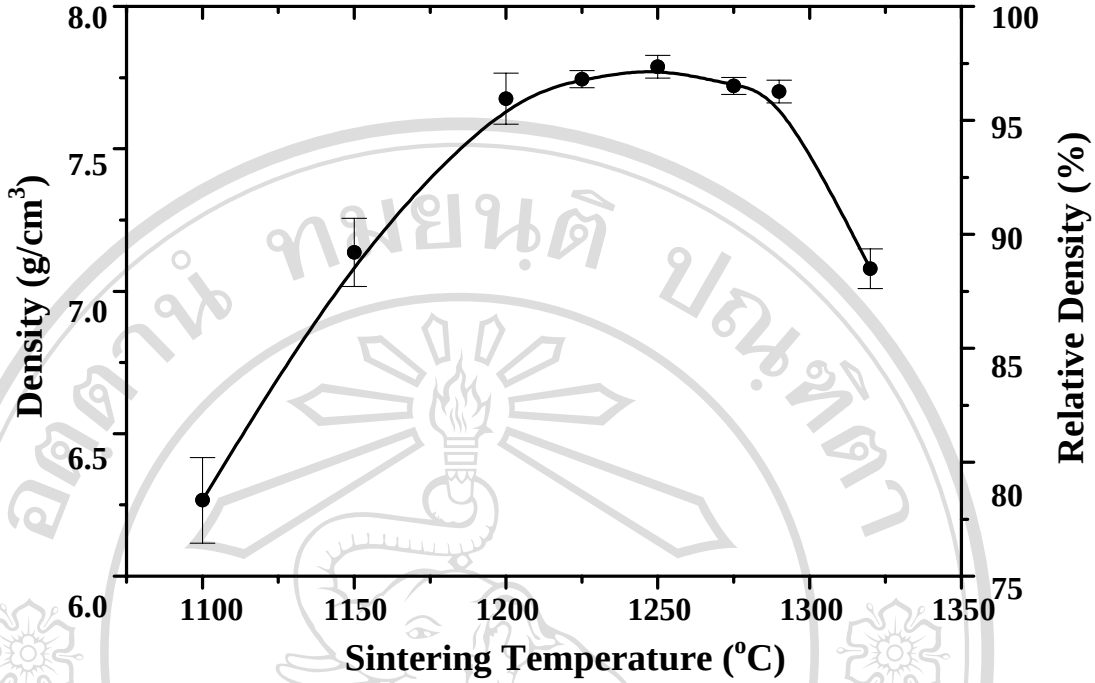

Fig. 4.18 Variation of density with sintering temperature for PZT ceramics sintered for 4 h with heating/cooling rates of 10 ^{o}C/min.

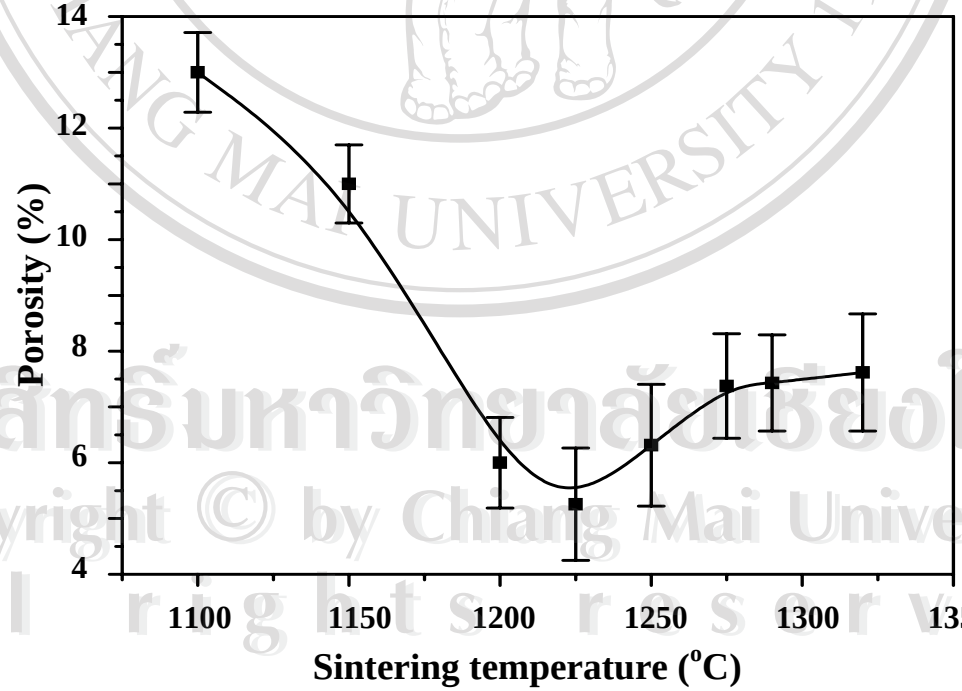

Fig. 4.19 Porosity versus sintering temperature for PZT ceramics sintered for 4 h with heating/cooling rates of 10 ^{o}C/min.

After powder pressing and sintering, a porous network is normally formed by the spaces between the necked powders. Here, the porosity is also plotted as a function of sintering temperature (Fig 4.19). It decreases with increasing sintering temperature from 1100 to 1225 ^{o}C, where it reachs a minimum of ~ 5.5 % which is close to the temperature that gives a peak value of the density. This is followed by a rising in porosity when sintered above 1225 ^{o}C. These results indicate that the tendency of porosity is almost an inverse of the density. Thus, densification behaviour of the PZT ceramics is clearly observed by the result of densities and porosity measurements.

However, the slightly increase of the porosity is observed for the temperature higher than 1275 °C which may be also corresponded to the decrease of the density of the sample sintered at the same temperature range. This observation may be attributed to evaporation of PbO at a high temperature range which the result can be seen as increase of porosity and decrease of density. This volatility of PbO leads to unbalanced stoichiometry as reported by Megriche et al.[106] Moreover, this result may also correspond to the presence of ZrO_2 observed by SEM (Fig. 4.15). Small segregation of ZrO_2 is seen as a second phase observed by XRD and SEM, mostly in connection with pores.[108]

The effect of PbO loss on an increasing of porosity can be understood from in-equilibrium of the PbO-vaporization/PbO condensation reaction which higher vaporization rate can take place at a higher temperature and is responsible for production of some open pores. This is consistent with the report of Bourtarfaia [108] and supports the hypothesis that ZrO_2 segregation is mainly originated from the vaporization of PbO.[108]

In Fig. 4.20, shrinkage increases in the initial period with sintering temperature. The optimum of linear shrinkage of PZT may be obtained at 1225 ^{o}C because this sintering temperature also gives a minimum porosity. From these results, it is proposed that the solid-state sintering mechanism take place at temperature between 1100-1225 °C which leading to a higher density, minimum porosity and higher shrinkage. At the temperature range 1250-1290 °C, shrinkage tends to decrease but weight loss still increase. This may be attribute to loss of Pb content at the surface which produces more open pores. These open pores do not effect the density values because of water filling-up effect during the measurement but they lead to lower shrinkage. With further increasing temperature to 1320 °C, the density decrease gradually while shrinkage is increased again. This is because of more loss of Pb and the loss may distribute throughout the whole bulk of the sample. Evidence of PbO volatilization which is seen as open pores is clearly visible and this has been confirmed by the SEM micrographs (Fig. 4.21).

Weight loss data of samples sintered at temperatures from 1150 ^{o}C to 1290^{o}C for 4 h are also shown in Fig. 4.20. It can be seen that in general, weight loss increases with sintering temperature. However, there is a marked sensitivity of weight loss above 1200 ^{o}C (> 1%). Weight loss was calculated by recording the weights of the samples before and after sintering. Thus, the observed rising in weight loss after sintering process could be attributed mainly to PbO volatilisation. However, there is no obvious relation between weight loss and density results.

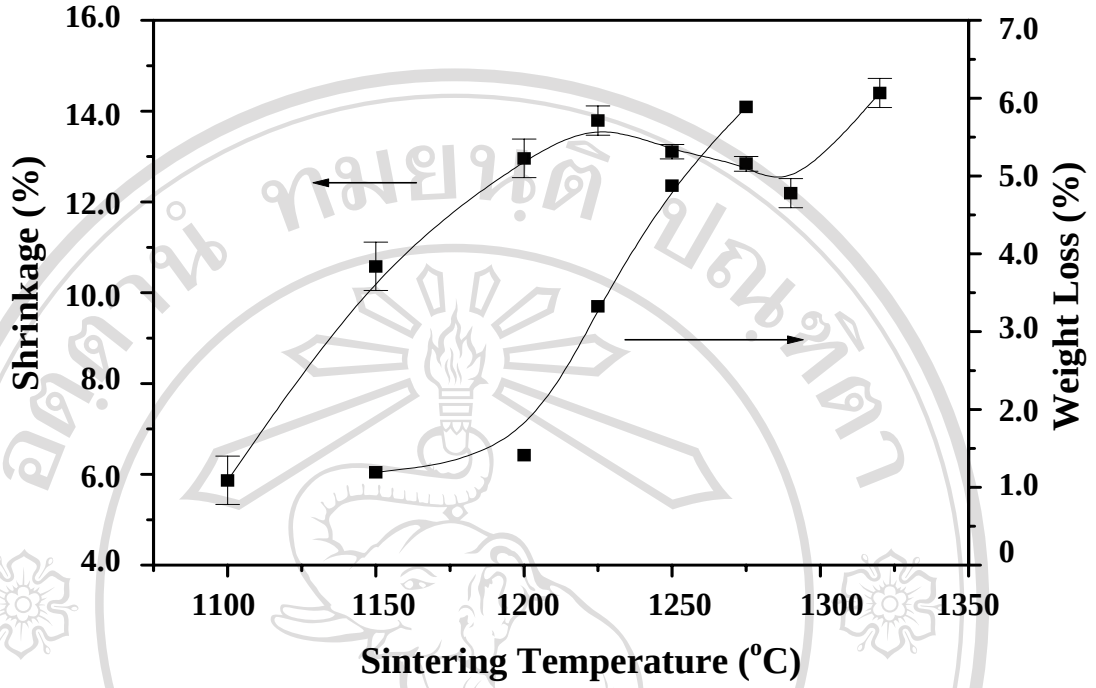

Fig. 4.20 Dependence of shrinkage and weight loss on sintering temperature for PZT ceramics.

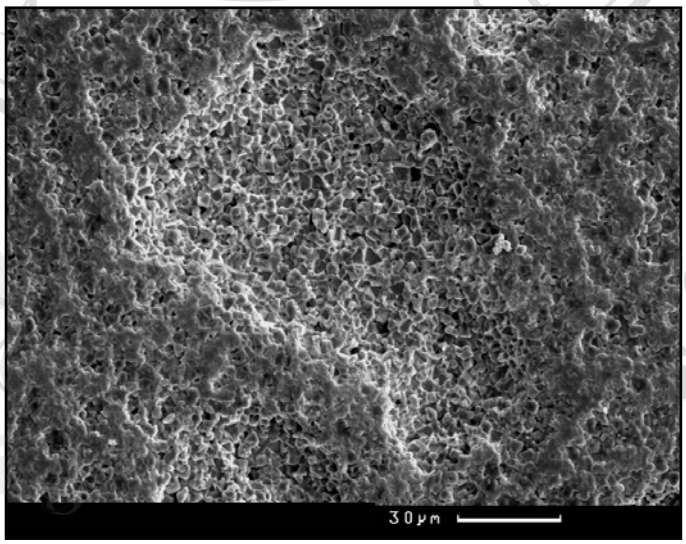

Fig. 4.21 SEM micrograph of PZT surface sintered at 1320 °C for 4 h with heating/cooling rates of 10 °C/min.

Microstructural development during sintering was investigated by scanning electron microscopy (SEM). Free and fracture surface micrographs of PZT ceramics sintered at various temperatures from 1150 ^{o}C to 1320 ^{o}C are shown in Fig. 4.22. In general, the results indicate that grain size tends to increase with sintering temperature, in agreement with other work.[37] The microstructure becomes denser as the sintering temperature increase up to 1250 ^{o}C, as indicated by the grain packing and increases in grain boundary thickness. A high sintering temperature (above 1225 ^{o}C) allows to obtain a relative sintered density of ~ 97% proving the good sinterability of these samples without going through the hot-pressing technique.

Several large pores with a broad presence of micro and meso porosity, are found in the samples sintered at lower temperature (Fig. 4.23), while very few small pore redius and narrow size distribution are found in samples sintered above 1225 ^{o}C. This small porosity value leads to the presence of a closed porosity formed during sintering process. The small pores with the average radius of 0.3 μm can be attributed to the porosity coming from powder packing process while the pores with the average radius of 2.5 μm are the result of decomposition reaction of PVA added as binder. As shown in Fig. 4.22, increasing the sintering temperature the small pores disappear giving rise to a few pores with radius of about one order of magnitude higher. The degree of porosity is controlled by the degree of partial sintering, which, in turn, is controlled by sintering at different temperatures and/or different times.

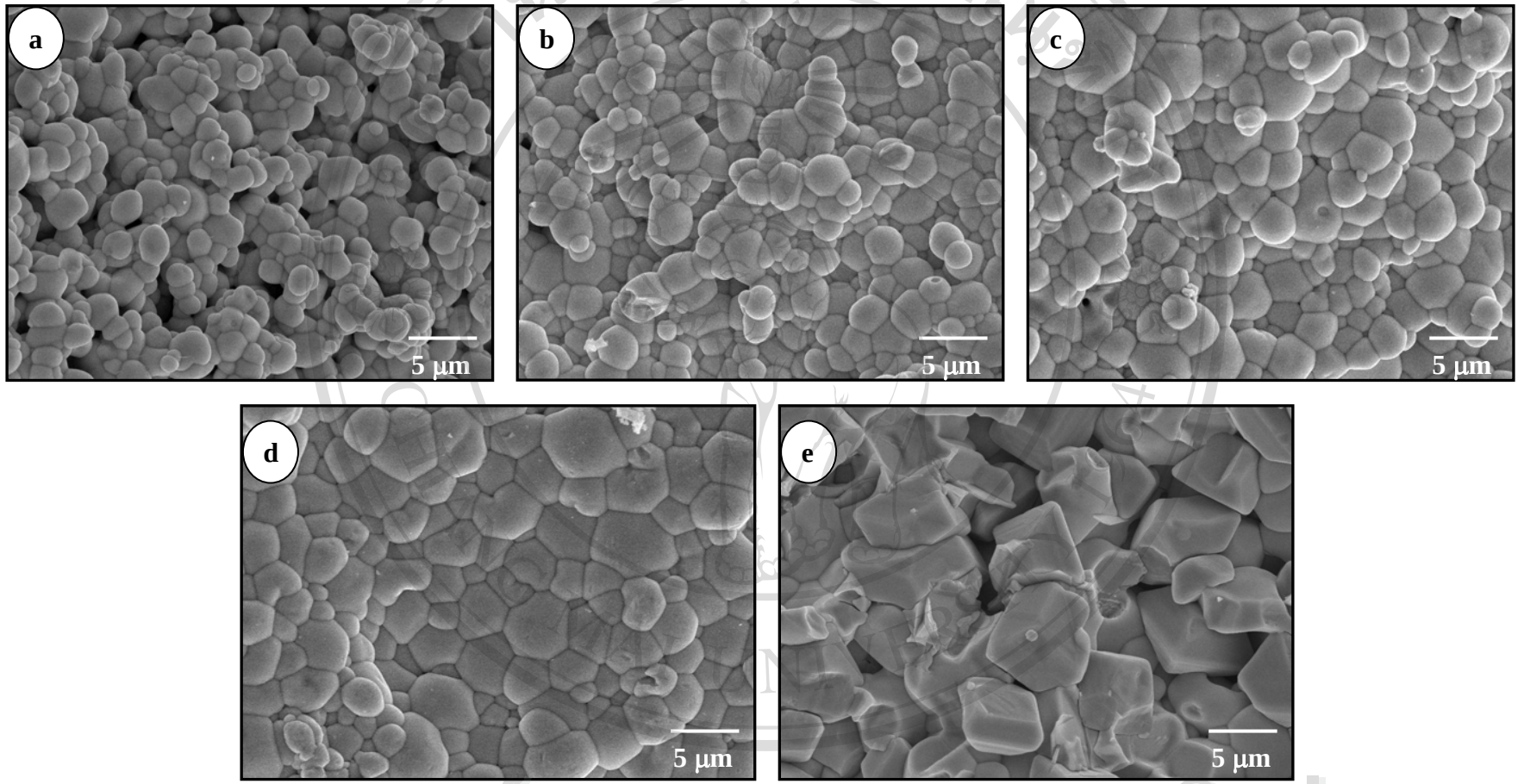

Fig. 4.22 SEM micrographs of free surface of PZT ceramics sintered at (a) 1150 ^{o}C, (b) 1200 ^{o}C, (c) 1225 ^{o}C, (d) 1250 ^{o}C and (e) 1320 ^{o}C.

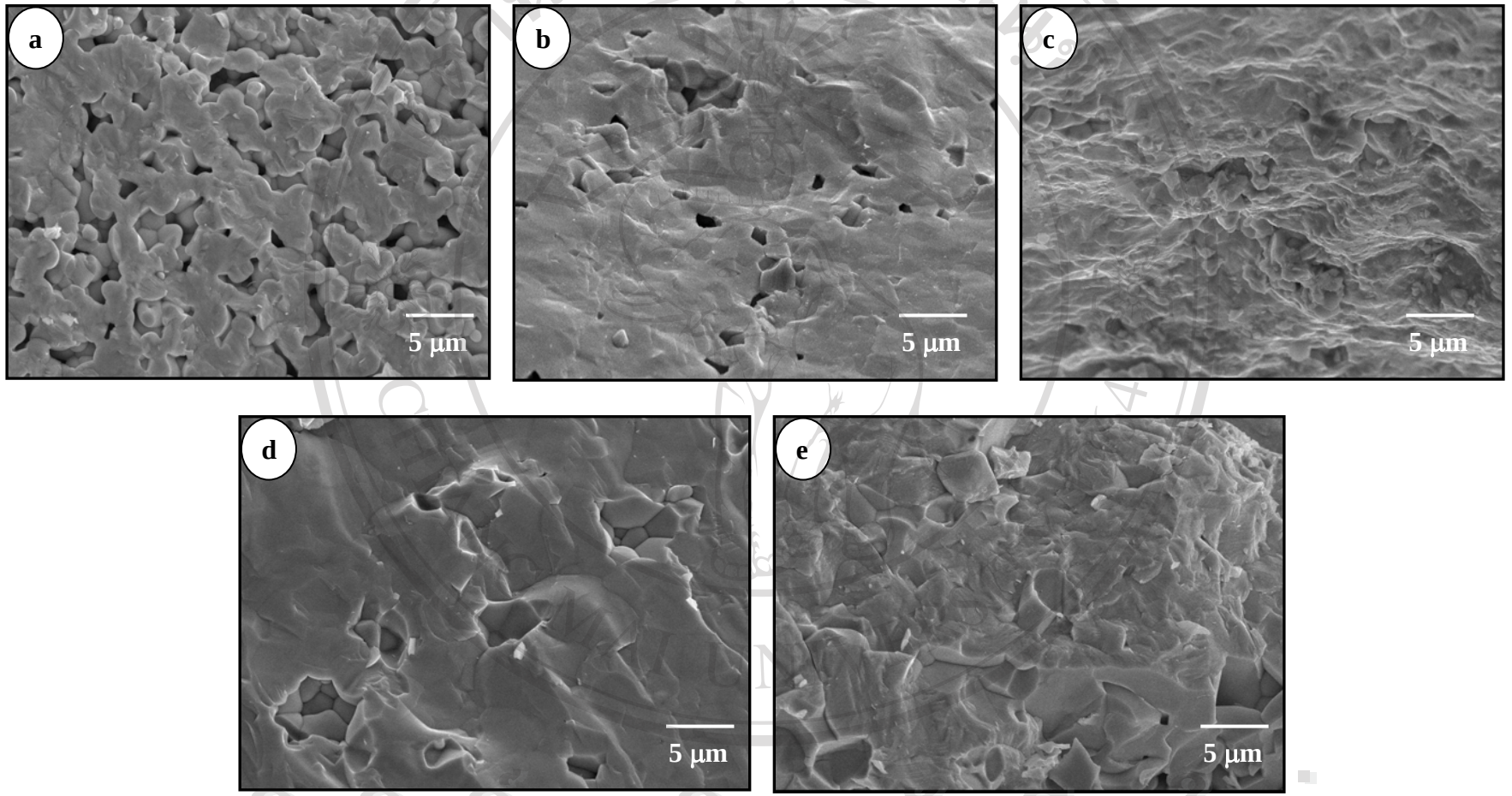

Fig. 4.23 SEM micrographs of fracture surface of PZT ceramics sintered at (a) 1150 °C, (b) 1200 °C, (c) 1225 °C, (d) 1250 °C and (e) 1320 °C.

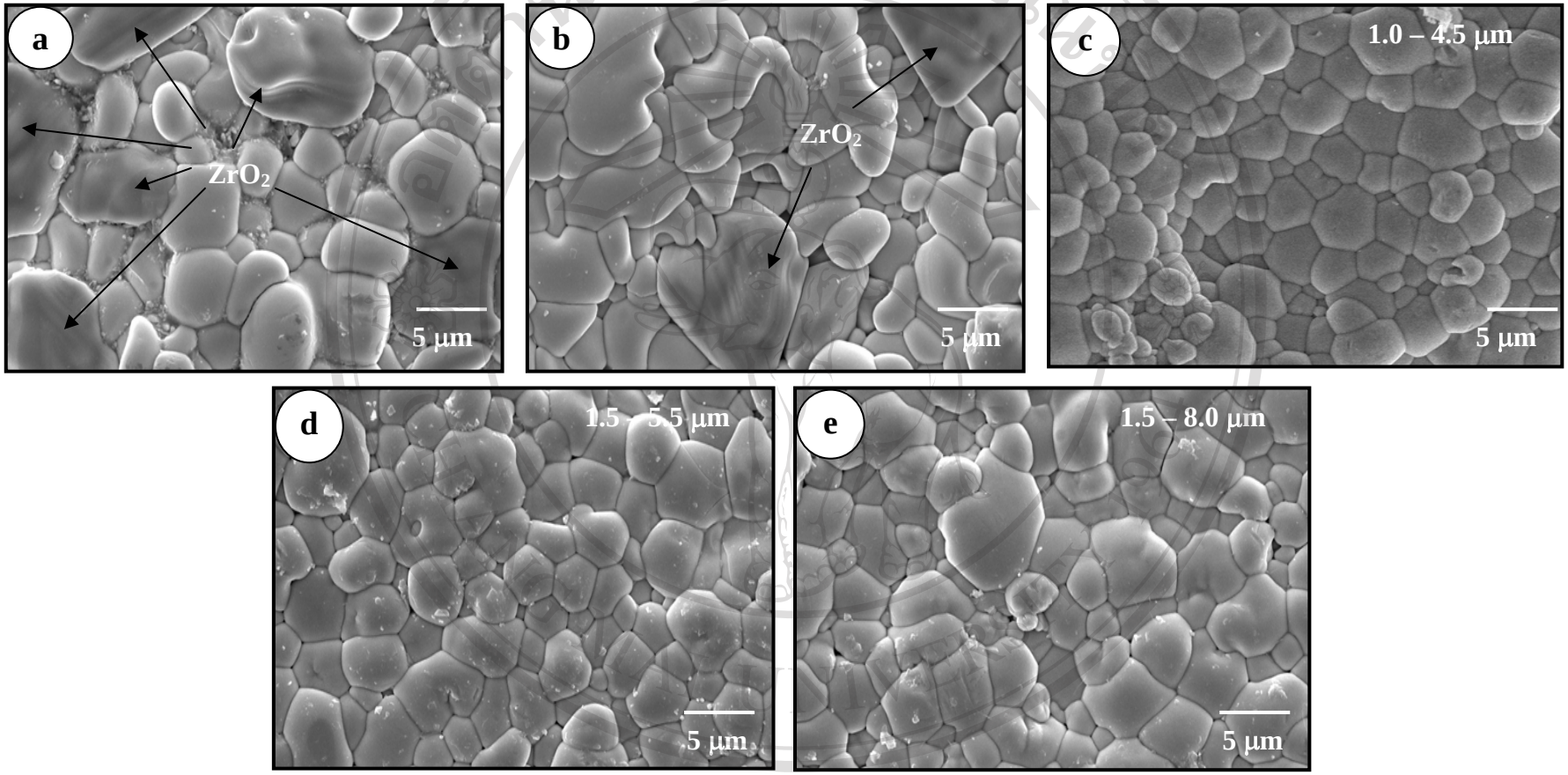

Fig. 4.24 SEM micrographs of PZT ceramics sintered at 1250 ^{o}C for 4 h with heating/cooling rates of (a) 1, (b) 5, (c) 10, (d) 20 and (e) 30 ^{o}C/min.

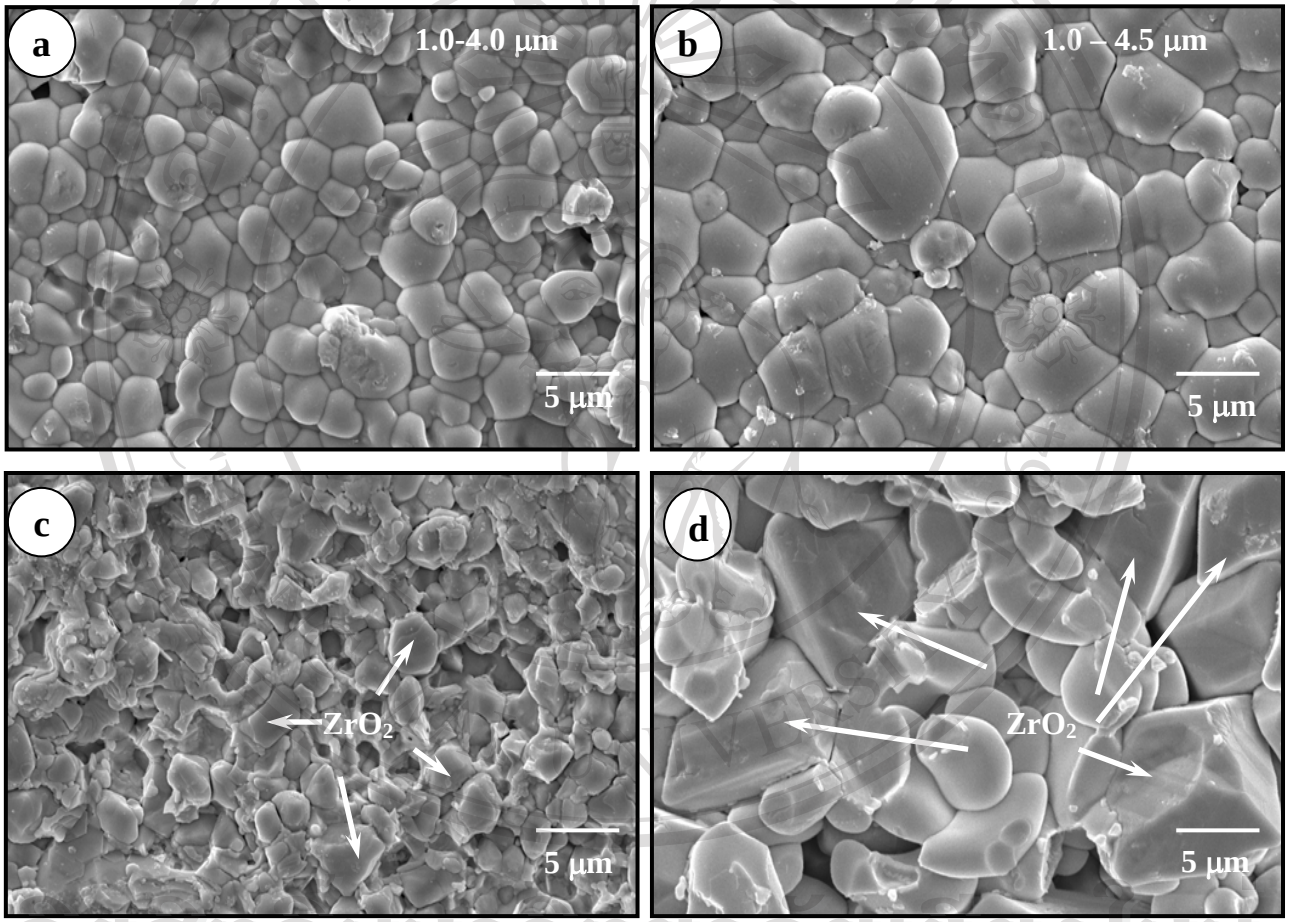

Fig. 4.25 SEM micrographs of PZT ceramics sintered at 1250 ^{o}C for (a) 2, (b) 4, (c) 6 and (d) 8 h with heating/cooling rates of 30 ^{o}C/min.

In this work, cracks or microcracks are not observed in the samples sintered from 1150 ^{o}C to 1225 ^{o}C. The increasing of grain sizes with increasing sintering temperature is clearly noticeable in this temperature range (Fig. 4.22). Samples sintered at 1200-1250 ^{o}C show a higher dense ceramics with larger grains of various sizes, i.e. 0.5-3.0 μm, 0.5-4.0 μm and 1.0-4.5 μm, respectively. From the present results, neither composition nor sintering temperature seems to have significant effect on the densification and microstructural development of PZT ceramics.

In this work, an attempt was also made to sinter PZT ceramics under various heating/cooling rates (Fig. 4.24) and dwell times (Fig. 4.25). When heating/cooling rates were varied from 1 to 30 °C/min, there are two distinctive grain shapes: i) irregular shape for the slower rates (2 and 5 °C/min), and ii) uniform grain shape for the faster rates (10-30 °C/min). Irregular and non-uniform grain shape observed at slow heating/cooling rates may be the result of longer sintering times that cause a higher degree of PbO evaporation. This also induces precipitation of the secondary phase which is clearly seen in the SEM micrograph (Figs. 4.24 (a) & (b)). EDS analyses show that sample compositions are inhomogeneous and the secondary phase is ZrO_2. Precipitation of ZrO_2 due to PbO deficiency was also reported by Garg and Agrawal[37] for PZT prepared by conventional method. However, presence of the ZrO_2 at the slow heating/cooling rates was not found by XRD measurement (see section 4.3.1). This is probably because of the limitations of the XRD technique. It is to be noted that samples heated and cooled at the rate higher than 10 ^{o}C/min show a higher uniform arrangement of the grains and no appearance of the secondary phase. The estimated grain sizes are in range 1.0-4.5 μm, 1.5-5.5 μm and 1.5-8.0 μm for heating/cooling rates of 10, 20 and 30 °C/min, respectively.

Micrographs of PZT ceramics sintered at 1250 ^{o}C for various dwell times are shown in Fig. 4.25. For the dwell time of 2 h, PZT grains still small with some pores still present. Grain growth to about 1.5-8.0 μm can be clearly seen with a higher densification when dwell time is about 4 h. For the longer dwell time, i.e. 6-8 h, presences of the ZrO_2 are distinctly observed with higher porosity compared to shorter dwell time. This means that the longer dwell time tend to produce more evaporation of the PbO content which in consequence promote pores and segregation of the ZrO_2 as observed previously for the higher sintering temperature.

Dark-field TEM image from PZT ceramic sintered at 1225 ^{o}C for 4 h is shown in Fig. 4.26 (a). Planar defects (arrowed) are observed which exhibit ribbonlike contrast, consistent with the presence of translational domain boundaries. Typical wedge-shaped ferroelastic twins are found. The grain is made of elongated domains visible as stripes of about 40-80 nm. The corresponding selected area electron diffraction (SAED) patterns from three grains at triple junction in sample show their tetragonal indexation. The strongest reflections in all patterns may be indexed according to a simple perovskite structure. For grains marked A and C (Fig. 4.26 (b) & (d)), superlattice reflections are present. These reflections are weak and diffuse (arrowed), suggesting that the amplitude and the correlation length of in-phase tilted regions are short. In addition, there is likely to be a contribution to the intensity of the $1/2\{hkl\}$ reflections arising from 1:1 ordering between the Zr and Ti cations. However, it is difficult to distinguish between these two mechanisms of superlattice formation using electron diffraction since double-diffraction of antiphase tilt reflections often results in the appearance of forbidden reflections which are

coincident with those associated with ordering. For grain B, no superlattice reflections are observed in <130> zone (Fig. 4.26(c)).

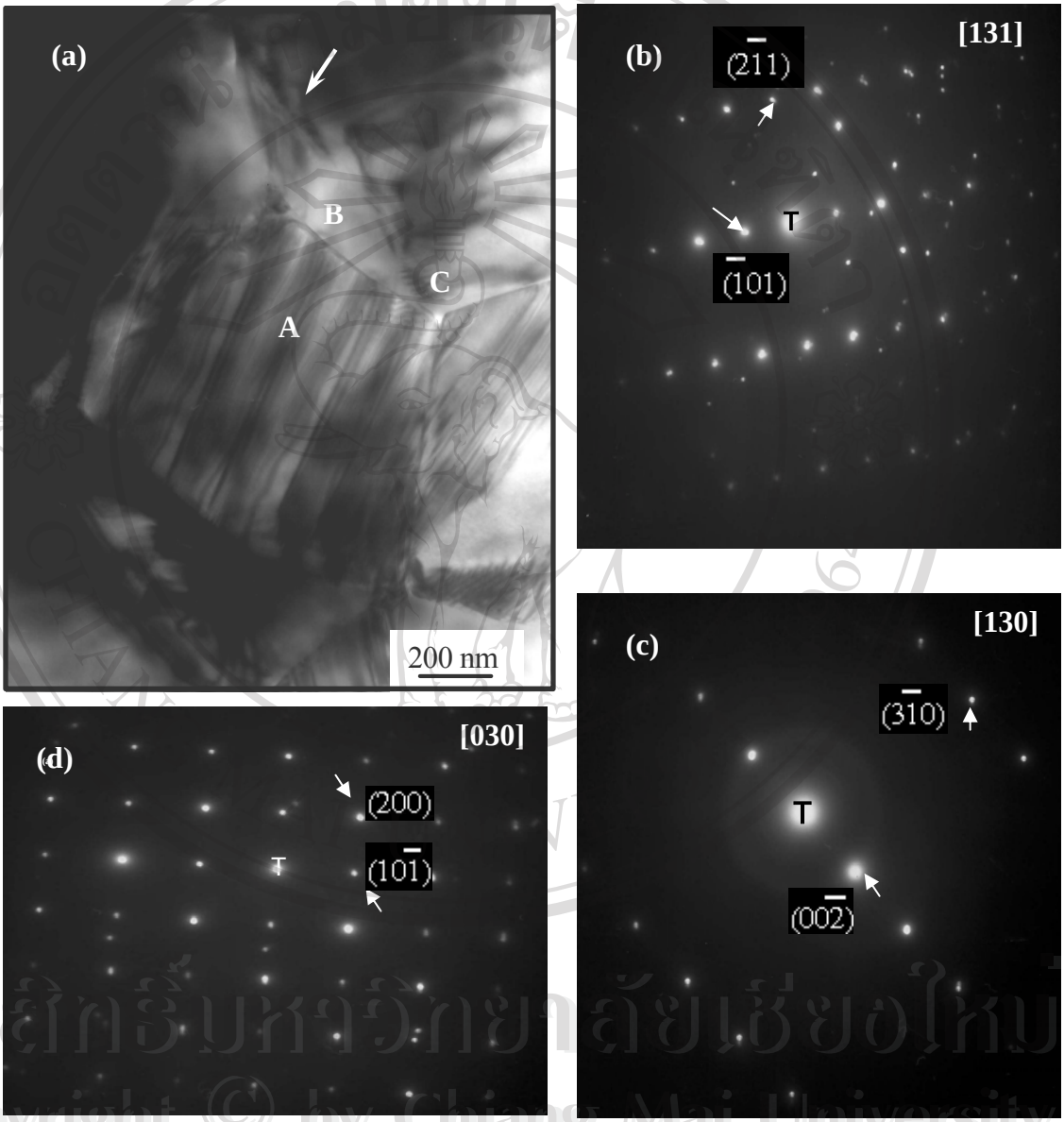

Fig. 4.26 TEM micrograph showing (a) dark-field images from grains of PZT ceramics and (b), (c) and (d) are the corresponding selected area electron diffraction (SAED) patterns of grains A, B and C, respectively.

In summary, for various sintering conditions, the densification and microstructure of PZT ceramics are disturbed by presence of the ZrO_2 impurity and appearance of pores due to loss of PbO especially at high temperature or long sintering time. In order to obtain optimized PZT ceramics, loss of PbO and precipitation of ZrO_2 have to be minimized. This work demonstrated that single phase of PZT ceramics with high density may be fabricated by employing a sintering temperature of 1225 ^oC for 0.5 h, with heating/cooling rates of 30 ^oC/min. The resulting PZT ceramics consist of variety of grain shapes and sizes, depending on sintering conditions.

4.3.3 Dielectric Properties

To determine the dielectric properties of PZT ceramics sintered at various temperatures, the dielectric constant and dissipation factor values as functions of temperature and frequency were measured using the LCZ measurement, as shown in Fig. 4.27. For all samples, it can be seen that the plots show similar peak characteristics at the Curie temperature. The frequency dependence of the dielectric constant was low. In general, the value of the dielectric constant decreased as frequency increased. The temperatures at the dielectric maximum ($\varepsilon_{r,\,max}$) are assigned as the T_c (Curie temperature). The results suggest that the T_c of all samples are approximately in range 298-377 °C. All the dielectric plots also obey the Curie-Weiss law[1] just above the peak temperatures. However, there are at least two regions of the T_c characteristics that can be observed. For samples sintered at 1150-1200 ^oC, T_c is rising with increasing density which could be attributed to the effect of pore

elimination from bulk ceramics as proposed by Akbas et al.[109] The fully dense PZT ceramic shows the T_c at about 385 ^oC. In contrast, for the samples sintered above 1200 ^oC, the T_c decreases to 377 ^oC. These observations may be a result of the internal stresses originated from the lattice distortion between ferroelectric and paraelectric phases. This is because ferroelectric behaviour is limited to the type of materials and only to a particular temperature range, in consistent with other work.[110, 111] It is to be noted that dissipation factor of all samples increases rapidly at the temperature closed to the T_c and the onset temperatures are also depended on frequency. The difference in dielectric properties at high temperature (> 400 ^oC) may be attributed to a space charge. Dependency of dielectric constant on sintering temperature may be accounted by the microstructural change of sintered PZT ceramics with increasing temperature, the same tendency as observed in density and grain size results, reported earlier.

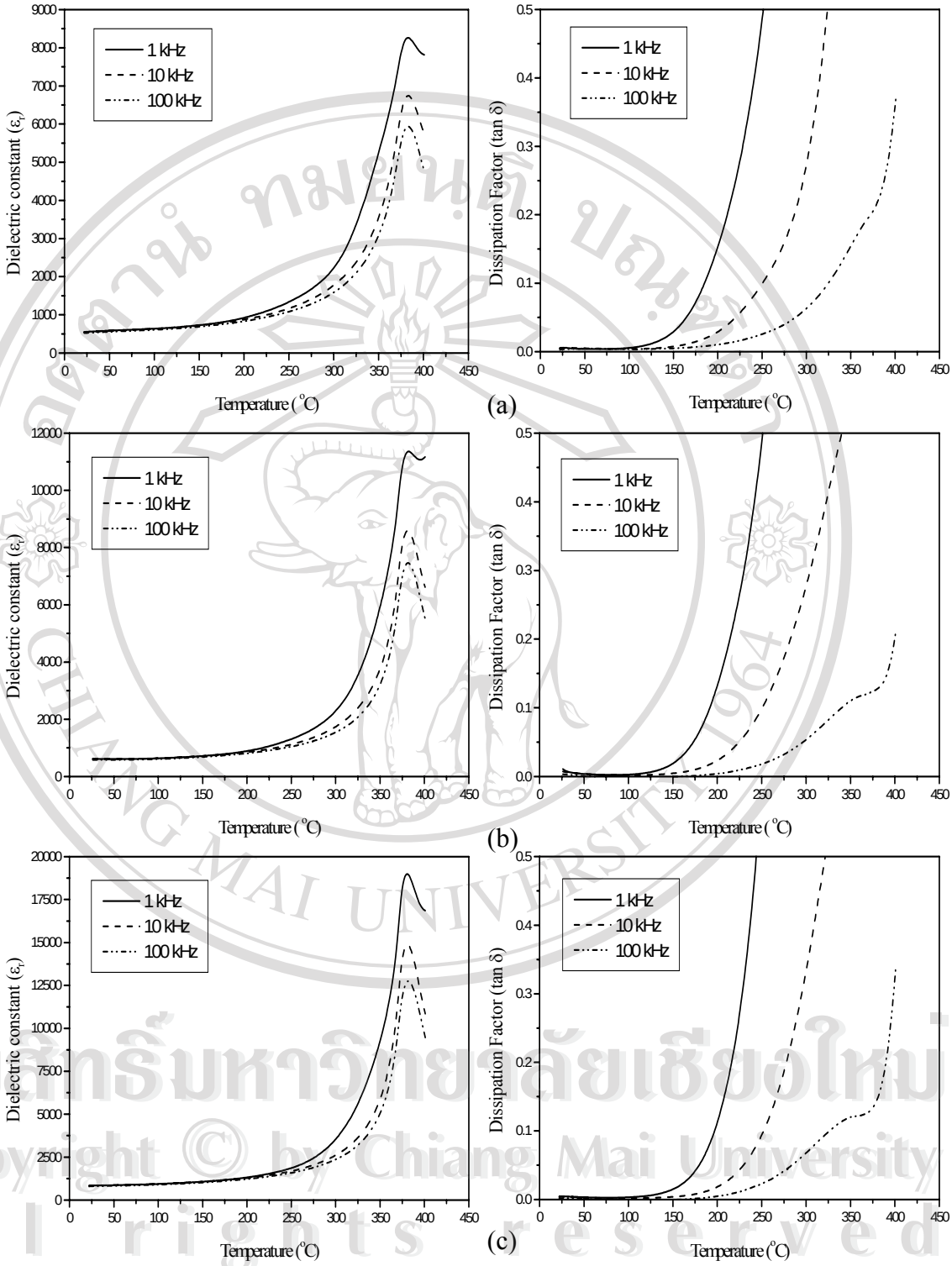

Fig. 4.27 The temperature dependence of the dielectric constant and dissipation factor of PZT ceramics sintered at (a) 1150 °C, (b) 1200 °C, (c)1225 °C, (d) 1250 °C and (e) 1275 °C, for 4 h with heating/cooling rates of 10 °C/min.

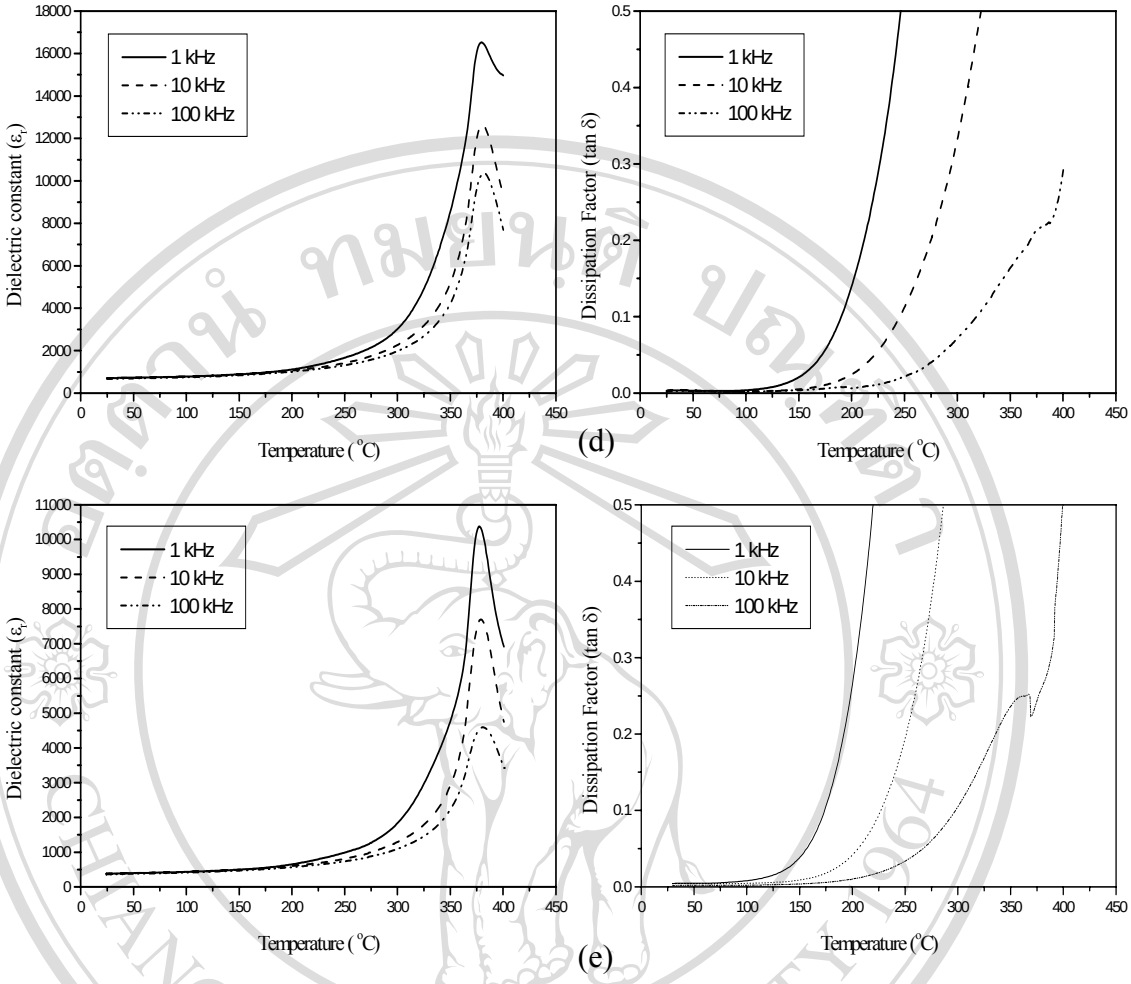

Fig. 4.27 (Continued)

Table 4.5 presents the dielectric constant and dissipation factor at room temperatures, Curie temperatures (T_c) and the averaged grain size, for the investigated samples sintered at various conditions. The maximum value of the dielectric constant at Curie point, i.e. about 18984 with a frequency of 1 kHz, is observed in the sample sintered at 1225 °C for 4 h. These results are in good agreement with the reported values for PZT ceramics.[25, 42, 109]

Table 4.5 Physical and dielectric properties of PZT ceramics sintered at various temperatures for 4 h with heating/cooling rates of 10 ^{o}C/min.

Sintering temperature (^{o}C)	T_c (^{o}C)	1 kHz				
		ε_r (T_R)	tan δ (T_R)	$\varepsilon_{r,max}$	tan δ_{max}	Average grain size (μm)
1100	298	550	0.0052	2177	1.55	/
1150	381	564	0.0072	8250	9.98	1.53
1200	385	638	0.0039	11316	3.99	1.84
1225	380	697	0.0038	18984	4.50	2.26
1250	379	463	0.0042	16524	4.35	2.76
1275	377	397	0.0047	10378	7.58	3.16

/ : data not available due to very highly porous ceramic was obtained.

Effect of the sintering temperature on grain size and dielectric properties is discussed here. The sintering temperature induced grain growth in the range 1.53-3.16 μm. It can be seen that as the grain size increases, the dielectric constant increases to a maximum at sintering temperature of 1225 °C, then decreases when the sintering temperature is further increased. The tendency of the dielectric constant variation is similar to that of density. This observation agrees with Kong and Ma's results,[112] only for the sintering temperature between 1100-1225 °C. Above 1225 ^{o}C, the dielectric constant does not increase but rather decrease even the averaged grain size of the ceramic still increase continuously with sintering temperature. In general, the dielectric constant is proportional to the grain size.[76] This means that the dielectric constant measured in this work is influenced by other factors. Inhomogeneity of the microstructure due to PbO deficiency and ZrO_2 precipitation at high sintering temperature may be responsible for the anomalous dielectric response observed here. Thus, the presence of pores and ZrO_2 impurity significantly reduces dielectric constant of the PZT ceramic.

In some cases of sintering conditions, the inhomogeneity of microstructure occurred. Evaporation of the PbO content is a major responsibility for the inhomogeinity. PbO deficiency also induces precipitation of ZrO_2 which is present as a secondary phase. This abnormal microstructure arrangement has effect on the densification of the PZT which is observed as anomalous densification for increasing of sintering temperature. The anomalous behavior observed in the PZT microstructure has considerably influenced its dielectric properties. However, fully dense PZT ceramics with 97% of the theoretical density have been achievable at a selected optimise sintering temperature, i.e. at 1250 ^{o}C for 4 h. This condition gives the

averaged grain size of 2.76 μm. By comparison, the measured values of the dielectric properties in the present work are in good agreement with the previous works of PZT ceramics prepared by different processing techniques.[42, 76, 107, 113]

Influence of the averaged grain size on the dielectric constant and dissipation factor at room temperature, 1 kHz for PZT ceramics is shown in Fig. 4.28. It was found that the dielectric constant and dissipation factor rise as the averaged grain size of PZT increases and become maximum at the average grain size ~ 3 μm. However, with further increases in grain size, the dissipation factor gradually decreases whilst the dielectric constant is quite independent on the averaged grain size. It is well established that the dielectric constant at room temperature of PZT ceramics is also highest near the MPB which may be a narrow band where two phases coexist.[114]

Grain size dependence of the maximum dielectric constant and its corresponding temperature at 1 kHz for PZT ceramics is shown in Fig. 4.29. In conventional PZT ceramics, it has been believed that smaller grains tend to clamp out extrinsic contributions such as domain wall motion.[1] However, in this work, it is seen that the dielectric properties fluctuation upon the varying average grain size of PZT ceramics is observed. This could be attributed to a number of key factors such as grain size distribution, purity, chemical homogeneity, Zr/Ti ratio, porosity and etc., which could not be under-estimated.

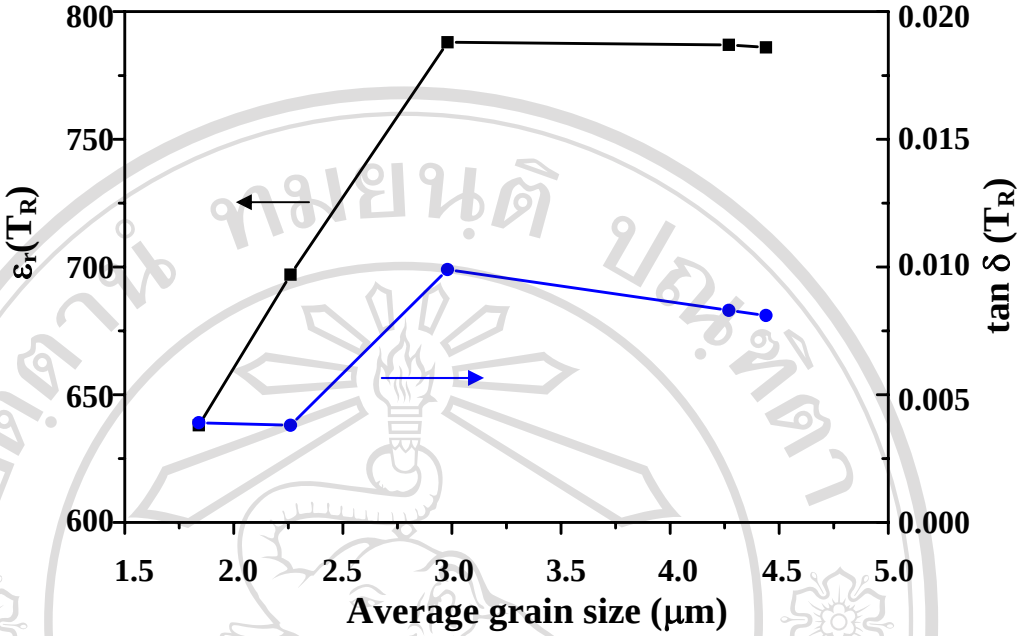

Fig. 4.28 The average grain size versus the dielectric constant and dissipation factor at room temperature.

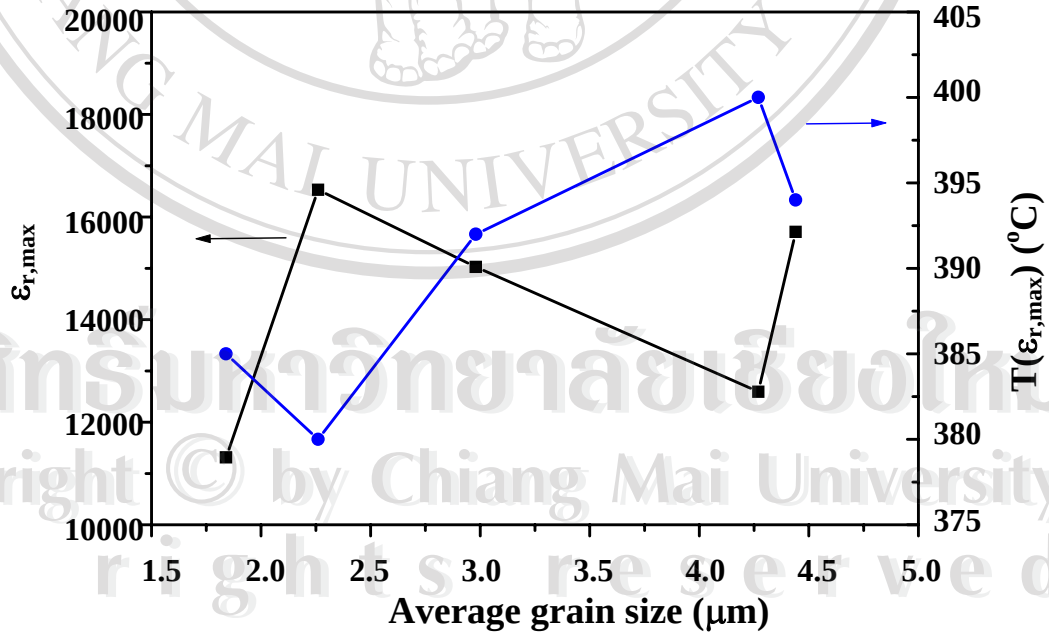

Fig. 4.29 The average grain size versus the maximum dielectric constant and $T(\varepsilon_{r,max})$ of PZT ceramics.